

Coupled chemistry climate model simulations of the solar cycle in ozone and temperature

J. Austin,¹ K. Tourpali,² E. Rozanov,³ H. Akiyoshi,⁴ S. Bekki,⁵ G. Bodeker,⁶ C. Brühl,⁷ N. Butchart,⁸ M. Chipperfield,⁹ M. Deushi,¹⁰ V. I. Fomichev,¹¹ M. A. Giorgetta,¹² L. Gray,¹³ K. Kodera,^{10,14} F. Lott,⁵ E. Manzini,¹⁵ D. Marsh,¹⁶ K. Matthes,^{16,17} T. Nagashima,⁴ K. Shibata,¹⁰ R. S. Stolarski,¹⁸ H. Struthers,⁶ and W. Tian⁹

Received 14 September 2007; revised 17 January 2008; accepted 26 March 2008; published 13 June 2008.

[1] The 11-year solar cycles in ozone and temperature are examined using new simulations of coupled chemistry climate models. The results show a secondary maximum in stratospheric tropical ozone, in agreement with satellite observations and in contrast with most previously published simulations. The mean model response varies by up to about 2.5% in ozone and 0.8 K in temperature during a typical solar cycle, at the lower end of the observed ranges of peak responses. Neither the upper atmospheric effects of energetic particles nor the presence of the quasi biennial oscillation is necessary to simulate the lower stratospheric response in the observed low latitude ozone concentration. Comparisons are also made between model simulations and observed total column ozone. As in previous studies, the model simulations agree well with observations. For those models which cover the full temporal range 1960–2005, the ozone solar signal below 50 hPa changes substantially from the first two solar cycles to the last two solar cycles. Further investigation suggests that this difference is due to an aliasing between the sea surface temperatures and the solar cycle during the first part of the period. The relationship between these results and the overall structure in the tropical solar ozone response is discussed. Further understanding of solar processes requires improvement in the observations of the vertically varying and column integrated ozone.

Citation: Austin, J., et al. (2008), Coupled chemistry climate model simulations of the solar cycle in ozone and temperature, *J. Geophys. Res.*, 113, D11306, doi:10.1029/2007JD009391.

1. Introduction

[2] The impact of solar irradiance variations on the atmosphere has long been seen as an important issue, and may have contributed to the Little Ice Age in the Northern Hemisphere during the Maunder minimum [Yoshimori *et al.*, 2005], although its more regional influence is still debated [Shindell *et al.*, 2003; Bengtsson *et al.*, 2006]. Indirectly, solar variations may have also contributed to decadal time scale variability in sea surface temperatures (SSTs) [White *et al.*, 2003]. In purely energetic terms, solar cycle variations are not significant, since for the 11-year solar cycle for example, the total solar irradiance varies by

only 0.08%. By the Stefan-Boltzman law, this can change the global temperature by only 0.06 K, which is too small to be detected. Therefore, if there is a solar impact on climate, then there must exist a process, or processes, which enhance the solar cycle or which is dependent on a part of the electromagnetic spectrum where the solar variation is larger. The suggestion of Haigh [1994, 1996], and supported by later calculations of, e.g., Shindell *et al.* [1999], is that stratospheric ozone could provide the important solar link to the tropospheric circulation by a modulation of the Brewer-Dobson circulation. Kodera and Kuroda [2002], Matthes *et al.* [2004, 2006] and Haigh and Blackburn [2006] have also demonstrated a link between the stratosphere and the

¹Geophysical Fluid Dynamics Laboratory, Princeton, New Jersey, USA.

²Laboratory of Atmospheric Physics, Aristotle University of Thessaloniki, Thessaloniki, Greece.

³PMOD/WRC and IAC ETHZ, Davos Dorf, Switzerland.

⁴National Institute for Environmental Studies, Ibaraki, Japan.

⁵UPMC Univ Paris 06, CNRS, SA-IPSL, B.102, Paris, France.

⁶NIWA, Omakau, Central Otago, New Zealand.

⁷Max Planck Institut für Chemie, Mainz, Germany.

⁸Met Office Climate Research Division, Devon, UK.

⁹Institute for Atmospheric Science, University of Leeds, Leeds, UK.

¹⁰Meteorological Research Institute, Ibaraki, Japan.

¹¹Department of Earth and Space Science and Engineering, York University, Toronto, Ontario, Canada.

¹²Max Planck Institute for Meteorology, Hamburg, Germany.

¹³NCAS Centre for Global Atmospheric Modelling, Meteorology Department, Reading University, Reading, UK.

¹⁴Graduate School of Environmental Studies, Nagoya University, Nagoya, Japan.

¹⁵Instituto Nazionale di Geofisica e Vulcanologia and Centro Euro-Mediterraneo per i Cambiamenti Climatici, Bologna, Italy.

¹⁶Atmospheric Chemistry Division, National Center for Atmospheric Research, Boulder, Colorado, USA.

¹⁷Institut für Meteorologie, Freie Universität Berlin, Berlin, Germany.

¹⁸NASA Goddard Space Flight Center, Greenbelt, Maryland, USA.

troposphere by a solar modulation of the polar night jet and the Brewer-Dobson circulation. The ocean response in sea surface temperature to solar variations can be another factor providing an amplifying link for the solar influence on the tropospheric circulation [Meehl *et al.*, 2003].

[3] Observations show a clear 11-year solar cycle in stratospheric ozone, both in the column [Zerefos *et al.*, 1997] and in its vertical distribution [Soukharev and Hood, 2006, and references therein; Randel and Wu, 2007; Tourpali *et al.*, 2007]. However, although model simulations have generally been able to simulate the response in the column amount reasonably accurately [Zerefos *et al.*, 1997], the vertical ozone profile has been in poor agreement with observations. For example, in low latitudes where the solar signal can be reasonably well established, the observations have a double maximum with near zero solar response near 10–20 hPa. In contrast model simulations both in two and three dimensions typically have simulated a response which increases with altitude and peaks near 10 hPa [Shindell *et al.*, 1999; Soukharev and Hood, 2006, Figure 14.]. Related differences between model simulations and observations also occur in the temperature response because of the radiative impact of ozone. Despite improvements in models, including the use of 3-D coupled chemistry climate models [e.g., Labitzke *et al.*, 2002; Tourpali *et al.*, 2003; Rozanov *et al.*, 2005b] these differences have tended to persist. All the aforementioned studies have completed two simulations by imposing fixed phase solar fluxes for solar maximum and solar minimum. In principle this procedure provided the largest atmospheric signal for the least computational cost. The results previously obtained therefore suggest either that the full solar cycle needs to be represented, or that there are missing processes in many of the simulations completed. For example, Callis *et al.* [2001] suggested that energetic electron precipitation generates NO_x in the upper mesosphere which then propagates to lower levels. Observations confirm this [e.g., Rinsland *et al.*, 2005] while the descent to lower levels is particularly rapid during stratospheric warmings [e.g., Manney *et al.*, 2008]. This process is generally restricted to high geomagnetic latitudes rather than low latitudes where a major model deficiency is noted. Langematz *et al.* [2005] were able to explain the middle stratospheric minimum by energetic electron precipitation, but these calculations are not supported by a more realistic description of the odd nitrogen source [Rozanov *et al.*, 2005a]. Also, the observational basis for the additional NO_x in the tropics is poor, with for example Langematz *et al.* simulating an amount about 3 times larger than observed [Hood and Soukharev, 2006].

[4] There are now some indications that the relatively poor model performance may have been resolved, if not understood. In recent simulations using coupled chemistry climate models, Rozanov *et al.* [2005c], Austin *et al.* [2007a] and Marsh *et al.* [2007] have been able to generate the observed minimum response in tropical ozone in the region 10–20 hPa assuming observed monthly varying forcings of SSTs and variations in solar flux on a monthly or daily frequency. In contrast, the ozone minimum response did not appear in simulations of the same models but with fixed phase forcing and climatological SSTs. For reasons that are not clear, two additional sets of simulations [Schmidt and Brasseur, 2006; T. Nagashima, personal

communication, 2007] now reproduce the observed ozone solar signal with fixed phase solar forcing in contrast to all other similar simulations known to the current authors, as presented for example in *World Meteorological Organization (WMO)* [2007, chapter 3], taken from Soukharev and Hood [2006]. In addition, the simulations of Schmidt and Brasseur [2006] used climatological SSTs.

[5] Most of the above models were used in the quadrennial ozone assessment [WMO, 2007, chapters 5 and 6]. Simulations of the different models were completed typically for the period 1960 to about 2000 or beyond with observed forcings, including observed SSTs and in some cases observed tropical winds. Most models also completed simulations for the future atmosphere. This work analyses the model runs of the past for the solar cycle and attempts to establish whether consistently improved model results are now obtained, as well as the possible reasons for this improvement. All the simulations include some or all of a number of processes affecting temperature and ozone, and to separate the various influences we employ multilinear regression as in the analysis of observations, particularly Soukharev and Hood [2006]. The current work continues the analysis of Eyring *et al.* [2006] which presented the model simulations and compared the results with observations for the basic atmospheric quantities temperature, ozone and other minor constituents. In addition we present a new analysis of the solar response in total column ozone prior to and during the satellite era from 1979 onwards.

2. Description of the 3-D Models and Simulations Included

2.1. General Description of Transient Runs

[6] The main model simulations included are denoted REF1 by Eyring *et al.* [2006], and are transient simulations for the period 1950 to 2004 or a subset thereof. All simulations are from fully coupled chemistry climate models extending to at least 0.1 hPa, although there are variations in the horizontal resolution and height domain, and details of the chemistry schemes used. As well as some of the basic model information, which also appears in Eyring *et al.* [2006], Tables 1 and 2 include additional information which could be of particular relevance to the solar cycle, such as an indication of the resolution of the radiation scheme, as given by the number of bands in the UV and visible. Of the simulations included, four model simulations (CMAM, GEOSCCM, LMDZrepo, UMSLIMCAT) did not include solar variations in the radiative fluxes. These simulations are included to provide contrasting results which in some respects might be interpreted as controls for the remaining simulations. Five models (AMTRAC, CMAM, GEOSCCM, LMDZrepo and WACCM) also did not include the quasi-biennial oscillation (QBO) in any form whatsoever, whereas the other models included a QBO either occurring naturally (MRI, UMETRAC, UMSLIMCAT) or with the tropical winds externally imposed in some form (CCSRNIES, MAECHAM4CHEM, SOCOL). The model simulations varied between single runs of 20 years and 3 runs of 54 years. Three models (AMTRAC, MRI and WACCM) were run as ensembles of 3, 5, and 3 members respectively to reduce the uncertainty in the derived model ozone signal.

Table 1. Model Names and References

Model	Name	Reference
AMTRAC	Atmospheric Model with TRansport and Chemistry	<i>Austin and Wilson</i> [2006] <i>Austin et al.</i> [2007a, 2007b]
CCSRNIES	Centre for Climate System Research National Institute for Environmental Studies	<i>Akiyoshi et al.</i> [2004]
CMAM	Canadian Middle Atmosphere Model	<i>Beagley et al.</i> [1997] <i>de Grandpré et al.</i> [2000]
GEOSCCM	Goddard Earth Observing System Chemistry Climate Model	<i>Bloom et al.</i> [2005] <i>Stolarski et al.</i> [2006]
LMDZrepro	Model of Laboratoire de Meteorologie Dynamique-Reactive Processes Ruling Ozone	<i>Lott et al.</i> [2005] <i>Lefèvre et al.</i> [1994, 1998]
MAECHAM4CHEM	Middle Atmosphere version of ECHAM4 with Chemistry	<i>Manzini et al.</i> [2003] <i>Steil et al.</i> [2003]
MRI	Meteorological Research Institute	<i>Shibata and Deushi</i> [2005] <i>Shibata et al.</i> [2005]
SOCOL	Solar Climate Ozone Links	<i>Egorova et al.</i> [2005] <i>Rozanov et al.</i> [2005a, 2005b]
UMETRAC	Unified Model with Eulerian TRansport And Chemistry	<i>Austin and Butchart</i> [2003] <i>Struthers et al.</i> [2004]
UMSLIMCAT	Unified Model SLIMCAT	<i>Tian and Chipperfield</i> [2005]
WACCM	Whole Atmosphere Community Climate Model	<i>Garcia et al.</i> [2007]

This permitted investigation into the sensitivity of the results to the analysis period. Only one of the models (WACCM) included the effects of upper atmosphere particle precipitation, and therefore in most cases the additional solar influence of NO_x suggested by *Callis et al.* [2001] is excluded. The simulations of MRI that are analyzed here, are primarily the new ensemble results with version 2, which included solar cycle changes in both the radiative heating and model photolysis rates. Some comparisons are made also with results from the model with version 1, which was a single simulation which appeared in *WMO* [2007, chapter 6] and which included the solar forcing only in the radiative heating. Comparisons are also made with a new version of AMTRAC. This is a single simulation and in the results here is denoted AMTRAC4. The model has undergone many improvements since *WMO* [2007]. The model ozone family scheme has been extended to the mesosphere and the convection scheme has been changed leading to higher and more realistic tropopause temperatures. Also, the chlorine parameterization has been adjusted leading to improved values in low and middle latitudes.

2.2. Solar Forcing in the Transient Runs

[7] Solar variability is forced explicitly in the models through changes in the radiative heating and photolysis rates. Details are included in the individual model descrip-

tions (references cited in Table 1) and also in *Eyring et al.* [2006]. Solar variability could also arise implicitly due to changes in the observed SSTs used as lower boundary forcing if those SSTs happened to be correlated with the solar cycle. Similarly, for those models which imposed a tropical wind, a solar response might arise implicitly if those winds are correlated with the solar forcing.

2.2.1. Photolysis Rates

[8] For most models, the photolysis rates are parameterized in terms of the monthly averaged 10.7 cm solar flux, although WACCM uses daily values. Most models represent photolysis rates with a look up table with base values calculated using a high resolution spectral model, typically 150 bands in the visible and ultraviolet (UV). An important term for the mesosphere and upper stratosphere is the inclusion of the Lyman- α band centered on 121.6 nm for the calculation of the photolysis rates. For this band, the solar fluxes typically increase by over 50% from solar minimum to solar maximum which can significantly influence the concentrations of CH_4 and H_2O [*Brasseur and Solomon*, 1987]. However, this is likely to have only a small impact on the results in the lower and middle stratosphere. The variation of the order of 10% in the Schumann-Runge and Herzberg regions also has a direct impact on ozone production in the middle atmosphere.

Table 2. Brief Description of Models and Simulations

Model	Simulations	Solar	Energetic Particles	QBO	Number of Radiation Bands and Spectral Coverage in UV/Visible
AMTRAC	3 × 1960–2004	Yes	No	No	14: 170–700 nm
CCSRNIES	1980–2004	Yes	No	Forced	7: 200–700 nm
CMAM	1960–2004	No	No	No	1: 250–680 nm
GEOSCCM	1960–2003	No	No	No	8: 200–700 nm
LMDZrepro	1979–1999	No	No	No	1: 250–680 nm
MAECHAM4CHEM	1980–1999	Yes	No	Forced	1: 250–680 nm
MRI	5 × 1980–2004	Yes	No	Internal	8: 200–700 nm
SOCOL	1980–2004	Yes	No	Forced	^a : 250–680 nm
UMETRAC	1980–1999	Yes	No	Internal	5: 200–690 nm
UMSLIMCAT	1980–1999	No	No	Internal	2: 200–690 nm
WACCM	3 × 1950–2003	Yes	Yes	No	8 ^b : 170–700 nm

^aIncludes an additional parameterization for solar effects [*Egorova et al.*, 2004].

^bIncludes special treatment for the shorter wavelengths [*Garcia et al.*, 2007].

2.2.2. Radiative Heating

[9] The photolysis rate changes caused by the solar irradiance variability can be reasonably well captured by the participating CCMs. However, it is less the case for the heating rates, because all the models use radiation codes from the core GCM, which were designed to attain the highest computational speed and in most cases no particular attention was paid to the solar variability effects. The ozone absorption in the spectral area 250–700 nm is responsible for about 90% of the heating rates in the stratosphere [Strobel, 1978]. However, because the solar irradiance variability changes are more pronounced for the shorter wavelengths [Krivova *et al.*, 2006], the direct radiative effects of the solar variability are formed in the stratosphere primarily by ozone absorption in the Herzberg continuum and in the mesosphere by the oxygen absorption in the Lyman- α line and Schumann-Runge bands. Therefore, the solar radiation code of CMAM, LMDZrepro and ECHAM4 (core GCM for MAECHAM4CHEM and SOCOL), which takes into account only ozone absorption in the 250–700 nm spectral interval, is fast and reasonably accurate, but its application for solar variability studies could lead to substantial underestimation of the direct radiative heating due to solar irradiance variability. This weakness has been confirmed by Egorova *et al.* [2004] and a parameterization has been added to the standard SOCOL radiation code to take into account the extra heating by ozone and oxygen due to solar irradiance variability. This deficiency in the ECHAM4/5 solar radiation code has also been illustrated by Nissen *et al.* [2007]. The solar radiation code of the UM (core GCM for UMETRAC and UMSLIMCAT CCMs) takes into account ozone absorption in the 200–690 nm spectral region. UMETRAC uses a more up to date code with more bands than UMSLIMCAT, but in both models some underestimation of the direct radiative heating response is expected only in the mesosphere due to the absence of oxygen absorption. The same is true for GEOSCCM, MRI and CCSRNIES models, which are able to treat the ozone absorption with the same spectral coverage. The more complex solar radiation code of AMTRAC takes into account the ozone and oxygen absorption in the 170–700 nm spectral region, and therefore the performance of this code should be better in the mesosphere. Of the models used here, WACCM has the most sophisticated solar radiation code, and the heating rates above the stratopause are derived from the photolysis rates calculated with high spectral resolution and wide spectral coverage. The latter approach (also implemented in the HAMMONIA CCM [Schmidt *et al.*, 2006]) can be recommended for future experiments aimed at the study of the solar irradiance effects. However, several technical issues need to be resolved before implementing this approach in operational models.

3. Regression Models

[10] For the zonally averaged ozone and temperature data as a function of pressure and latitude the following regression equation was assumed:

$$M(t) = \mu_j + a_0 + a_1 t + a_2 u_{30} + a_3 u'_{30} + a_4 F_{10.7} + a_5 A + \epsilon(t) \quad (1)$$

where $M(t)$ is the model quantity averaged for each season of the simulation, t is time in seasons, and μ_j is the seasonal average over all the years of the analysis, for the j th season. u_{30} is the equatorial wind at 30 hPa, $F_{10.7}$ is the 10.7 cm solar flux, and A is the aerosol surface area at 60 hPa at the equator estimated from the optical depth [Thomason and Poole, 1997]. The term u'_{30} has been constructed normal to u_{30} by copying u_{30} and shifting it in one day increments, using linear interpolation to derive values at sub-month resolution, until the time integral of $u'_{30}u_{30}$ was zero. The two wind fields have been normalized to an amplitude of 1 which then allows a phase lag between the dependent variable and the wind to be taken into consideration. A similar out of phase term was also included for the solar flux in earlier calculations but this led to steep phase gradients in the lower stratosphere in some cases, where the solar signal was small compared with the uncertainty. For simplicity therefore the solar phase lag is neglected, as indeed it is in the ozone analysis of Soukharev and Hood [2006]. The dependent variable is treated as first order autoregressive, AR(1), using the method of Tiao *et al.* [1990], so that the residual term $\epsilon(t)$ is taken to be of the form

$$\epsilon(t) = b\epsilon(t-1) + w(t) \quad (2)$$

where b is a constant and $w(t)$ is expected to be a white noise function. Equation (1) was solved for the coefficients a_i using the least squares algorithm developed for the NAG library [NAG, 1999]. The μ_j terms contain the seasonal variation and the a_i coefficients represent the secular variations which are discussed in this paper. The same regression model, given by equations (1) and (2) was also used for the total column ozone discussed in sections 4.4 and 5.

[11] The regression model is very similar to that of Soukharev and Hood [2006], but the main difference is that here we use 10.7 cm flux as the independent solar forcing term, as the photolysis rates in the models themselves were driven by these flux values. By contrast, Soukharev and Hood used the magnesium index for their solar forcing term. Since not all models have a tropical oscillation, the QBO cannot play a role in some of the simulations. Other variations in tropical dynamics may be contributing, and this is reflected by including u_{30} and u'_{30} as independent variables. By basing the regression model on that of Soukharev and Hood, the model results can be directly compared with their observational analysis. The regression equation includes a trend term a_1 . In principle this could represent changes due to all non-solar and non-aerosol photochemical processes including indirect processes arising from stratospheric cooling, but in practice chlorine change is the dominant process influencing a_1 . Clearly, the regression could be reformulated to add explicitly a chlorine term, but the results could not then be compared directly with Soukharev and Hood. Results for one of the models (AMTRAC) were also recomputed with a halogen term replacing the trend term and this was found to have a negligible effect on the solar coefficient a_4 . The aerosol term is included at all levels, but does not have a significant influence on the solar coefficient. A time lag is not included in the aerosol term even though its effects may take time to influence ozone and temperature. Much comment has been made in the literature and elsewhere concerning the aliasing

between the solar and aerosol terms. However, in this work removing the aerosol term entirely had only a small impact on the solar coefficients because there hasn't been a major eruption for the whole of the last solar cycle. Aliasing between the solar and other independent variables is generally of concern and in particular we comment later on the impact of u_{30} which is a proxy for the QBO. Also, in section 4.3, we consider the impact of an SST term in equation (1). An SST-term is also included in a regression expression by *Steinbrecht et al.* [2006] who focus on MAECHAM4CHEM and observations and consider also terms related to the strengths of the polar vortices.

[12] All models include sea surface temperature variations, which contribute to ozone variations indirectly via transport. However, the results obtained here were not generally found to be sensitive to the sea surface temperatures, except those models which started before 1980; see section 4.3. Hence it is not included in the regression equation. This also ensures consistency between the analysis of total column ozone, ozone vertical variability and the observations of *Soukharev and Hood* [2006].

[13] A similar analysis has been performed for the zonally averaged total ozone time series derived from observations available for the period 1964–2006 [WMO, 2007, chapter 3; V. Fioletov, personal communication, 2006].

4. Results: Ozone

4.1. Latitude and Pressure Variation of the Ozone Solar Cycle

[14] The latitude and pressure variation in the annually averaged model solar responses, $4a_4/(\mu_1 + \mu_2 + \mu_3 + \mu_4)$, for those models with explicit solar forcing is shown in Figure 1. The response is typically 1–2% in each model and a statistically significant response occurs in most models over a limited region above about 10 hPa. However, each model has a different signal, due amongst other things to model interannual variability. Large differences also occurred between the individual ensemble simulations of AMTRAC, MRIV2 and WACCM, but only the ensemble means are shown. Results from MRIV1 appeared in WMO [2007, chapters 5 and 6] and may be compared with results from MRIV2. In the former, solar cycle variations are included only in the radiative heating rates, whereas in the latter, the model photolysis rates also have a solar cycle. In the photochemically controlled region in the upper stratosphere, MRIV1 exhibits only a slight ozone solar cycle response as the simulations does not include the photochemical response. In the dynamically controlled region in the lower stratosphere, MRIV1 and MRIV2 give similar results due to the relative unimportance of photochemistry. AMTRAC4 is an additional simulation which is an improved version of AMTRAC, with a mesospheric ozone scheme, an improved gravity wave drag parameterization, and improved parameterization of Cl_y production rates. In high latitudes, the model results are less consistent with each other, although the uncertainty in the derived solar cycle is quite large even in the mean of the ensemble runs. In the tropical lower stratosphere, models have a distinct minimum in solar response, as analyzed in more detail in the next subsection.

[15] The results of Figure 1 may be contrasted with those obtained for the models without explicit solar forcing (Figure 2). As would be anticipated, these models do not generally imply a solar signal. A coherent signal is absent in all the models, except in the LMDZrepro results, which imply a possible statistically significant signal in the Antarctic lower stratosphere. In this region, no other model gives a response to the solar cycle of such a large magnitude. Because of several biases, Antarctic polar ozone in LMDZrepro is anomalously sensitive to the volcano-driven variations of aerosol loading. The sulfuric acid aerosol fields used in their simulations were taken from microphysical simulations using a global 2D chemistry/aerosol model using its own winds and temperatures. This procedure tends to overestimate the amount of sulfuric acid particles present at high latitudes during winter and spring because of the absence of a polar vortex barrier in the 2D model. The other problem in the LMDZrepro simulations is the negative temperature bias in the Antarctic lower stratosphere and hence the vertical, horizontal and temporal extent of PSCs is also anomalously large. Finally, in the LMDZrepro PSC scheme, the amount of chemical processing depends on the aerosol loading. These effects combine to make Antarctic polar ozone sensitive to the variations in aerosol loading and any aliasing between the aerosol and the solar cycle can be misinterpreted as a solar signal.

[16] The mean of all the model results is shown in Figure 3, broken down into those with solar forcing and those without. For the runs with solar forcing, a much more coherent vertical structure is present compared with the individual models, giving rise to a small latitudinal variation. In the tropics, ozone has a minimum response near 20 hPa. A minimum also occurs at other latitudes, but at a lower level. For the model simulations without explicit solar forcing, the mean solar response is about 0.5% per 100 units of $F_{10.7}$ but with a typical uncertainty of about twice as much. The apparent solar response increases in the tropical lower stratosphere as in the solar forced simulations, although the response is not statistically significant.

4.2. Low Latitude Average

[17] As indicated in Figures 1–3, most of the model simulations have a minimum in ozone solar response near 20 hPa. This feature has appeared in observations at a slightly higher level, about 10 hPa, but has proved difficult for models to simulate [e.g., *Soukharev and Hood*, 2006]. The difference between observations and models for the altitude of the minimum is probably not statistically significant bearing in mind the large uncertainties in determining the solar response. The monthly model results were first averaged over the latitude range 25°S to 25°N and the regression equations were then recomputed. The results are shown in Figure 4, together with satellite observations. Comparisons with observations are discussed in section 5.

[18] For those models which have explicit forcing (Figure 4, upper panels), the results are generally in agreement with each other, bearing in mind the large uncertainties of typically 1%/100 units $F_{10.7}$. The models indicate a clear minimum in solar response near 20 hPa. Those models without explicit solar forcing (Figure 4, lower left) have dramatically different results, with none of the models having a response significantly different from zero at any

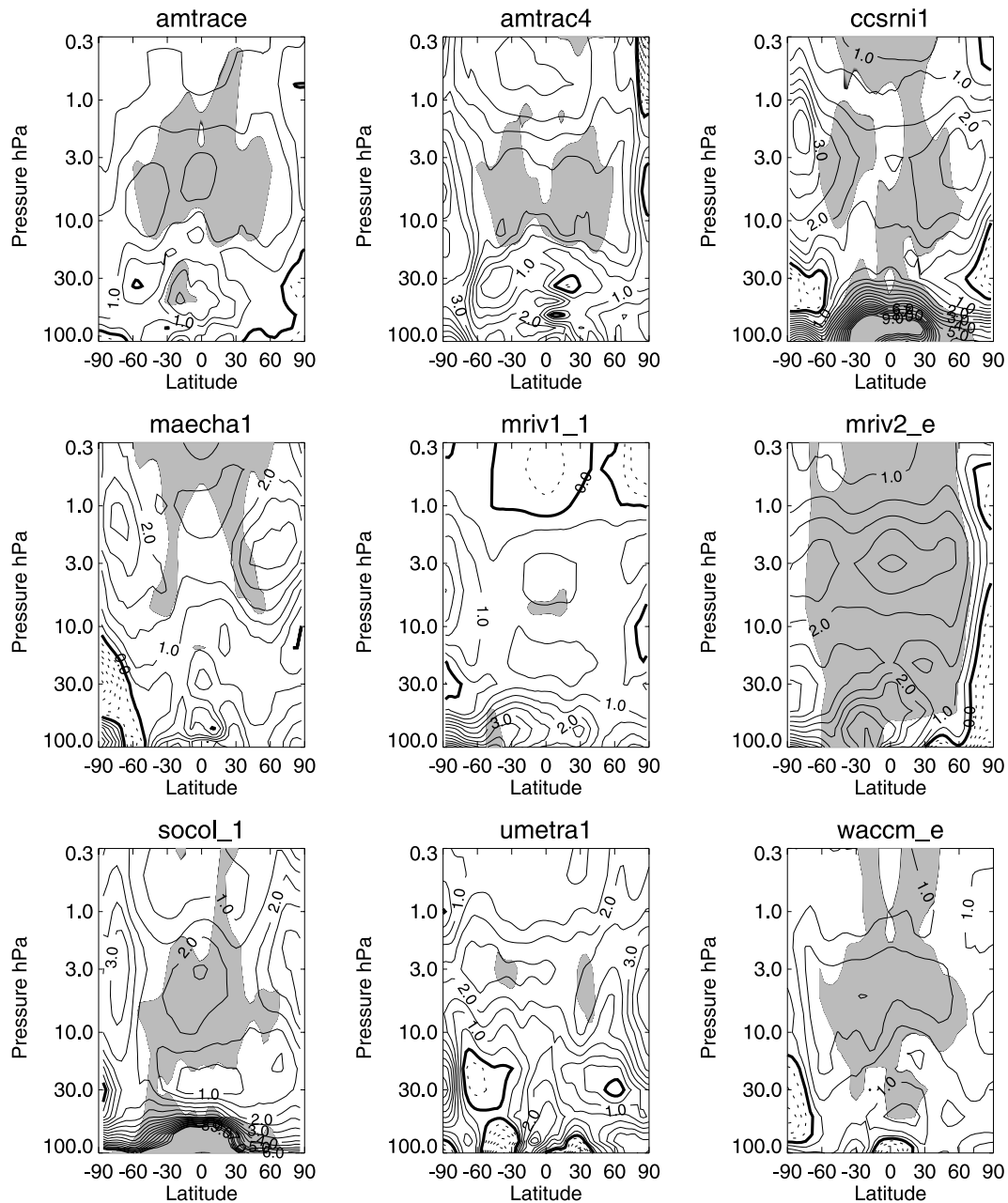


Figure 1. Annually averaged ozone solar cycle response (% per 100 units $F_{10.7}$), as a function of latitude and pressure, for those models which explicitly included solar forcing. The contour interval is 0.5 and the shaded region indicates where the solar response is significantly different from zero at the 95% confidence level. Contours with broken lines indicate negative contour values with the zero contour drawn in bold. The model names are indicated at the top of each panel, truncated to the first 6 characters. The 7th character refers to the simulation number for that model (typically 1), or *e* for the ensemble mean.

level. Some indirect solar response might have been present, if the lower atmosphere forcing were significant and driven by solar forcing of the observed SSTs, but in general for these models that does not appear to be the case, although see section 4.3. The simple mean of all the model simulations which had a solar forcing, is shown in Figure 4 (lower, right). The model and observation error bars overlap throughout the domain.

[19] It has been suggested that the QBO is important in determining the low latitude ozone solar response either by affecting the signal directly [McCormack, 2003; McCormack

et al., 2007], or due to a statistical interference in the signal [Lee and Smith, 2003]. Of those models which explicitly included solar forcing, most models also included some form of QBO, either internally generated or forced (see Table 2). In comparison, there were two models (AMTRAC and WACCM) which had explicit solar forcing but did not include any type of QBO. Examination of Figure 4 indicates that for the simulations presented in this work, there was no clear difference between those simulations including a QBO and those without one.

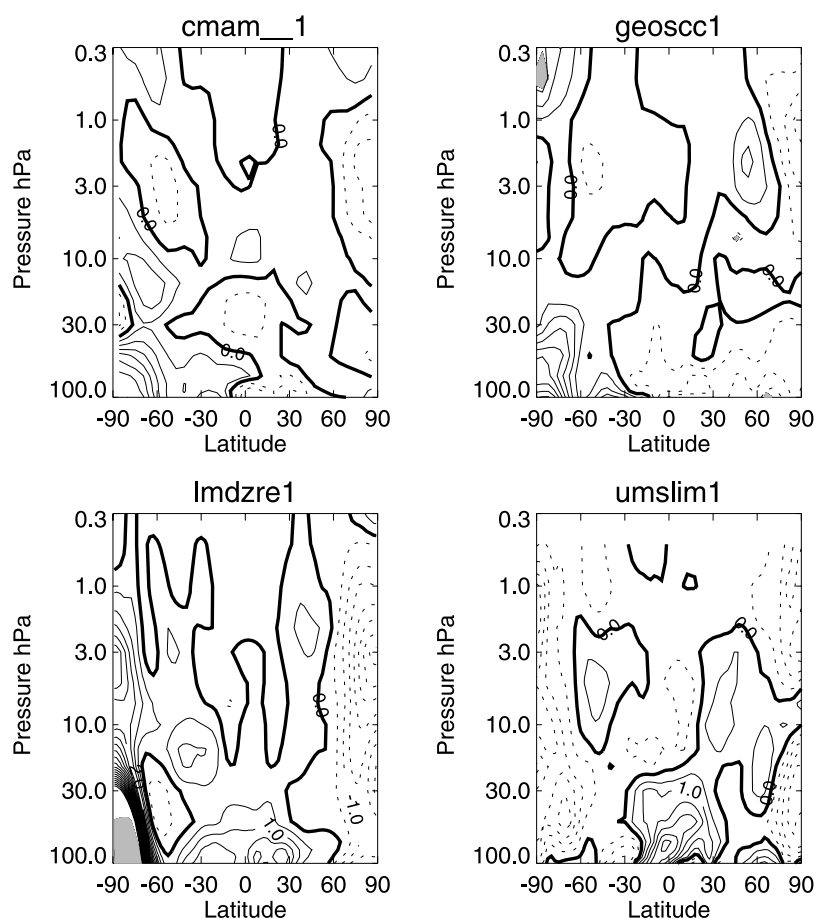


Figure 2. Annually averaged ozone solar cycle response (% per 100 units $F_{10.7}$), as a function of latitude and pressure, for those models which did not include explicit solar forcing. The contour interval and shading are the same as in Figure 1.

[20] For those runs which completed ensembles, the uncertainties are smaller than the other models and the minimum feature near 20 hPa in all the models is statistically more distinct from the maxima which occur higher and lower in the atmosphere (Figure 4, upper left). Both WACCM and AMTRAC are in agreement with each other throughout the pressure range up to about 1 hPa. Comparisons with the results of the improved AMTRAC run (not shown) indicate that the oversimplifications in the AMTRAC mesospheric chemistry scheme have contributed to most of the differences above 1 hPa. MRI results are qualitatively similar to the other two models, but the absolute values are about 50% larger, which is in better agreement with observations in the upper and lower stratosphere.

[21] Owing to the large volume of data from the ensemble runs of AMTRAC and WACCM, it is possible to compare the solar cycle for different periods and the results have been split into 1960–1981 and 1982–2003 for each model, covering six solar cycles in total in each period from three runs. All the other models which imposed a solar forcing were integrated from 1980 onwards. Results for the separate periods were also calculated for CMAM. Above 10 hPa, the results are not dependent on the time period in any of the models (Figure 5), but in the lower stratosphere the solar signal changed substantially. Although there are differences between AMTRAC and WACCM regarding the lower

stratospheric minimum feature, both models show a strong negative response in the lower stratosphere for the period 1960–1981, compared with a strong positive response from about 1982. Further, both models agree better with observations using the results of the later period rather than the earlier period, particularly in the lower stratosphere (see section 5). Despite the absence of a solar cycle in the CMAM forcing, the CMAM results also have similar features, albeit not statistically significant, of a negative response for the early period and a positive response for the later period when projected on to the solar forcing. In comparison, in the middle and upper stratosphere, the CMAM solar response is less than 0.5% for all the periods considered.

4.3. Sea Surface Temperature Impact on the Derived Solar Sensitivity

[22] SSTs influence tropospheric dynamics which in turn affect the ozone amount by vertical transport. In the above formulation of the regression equation, this has been neglected. To consider the SST effect, the regression calculation was repeated after adding an additional independent variable, which is the tropical mean SST, seasonally adjusted and averaged over the latitude range 22S to 22N. The SSTs were lagged by 18 months to allow the tropospheric processes to influence the results at the 30 hPa pressure

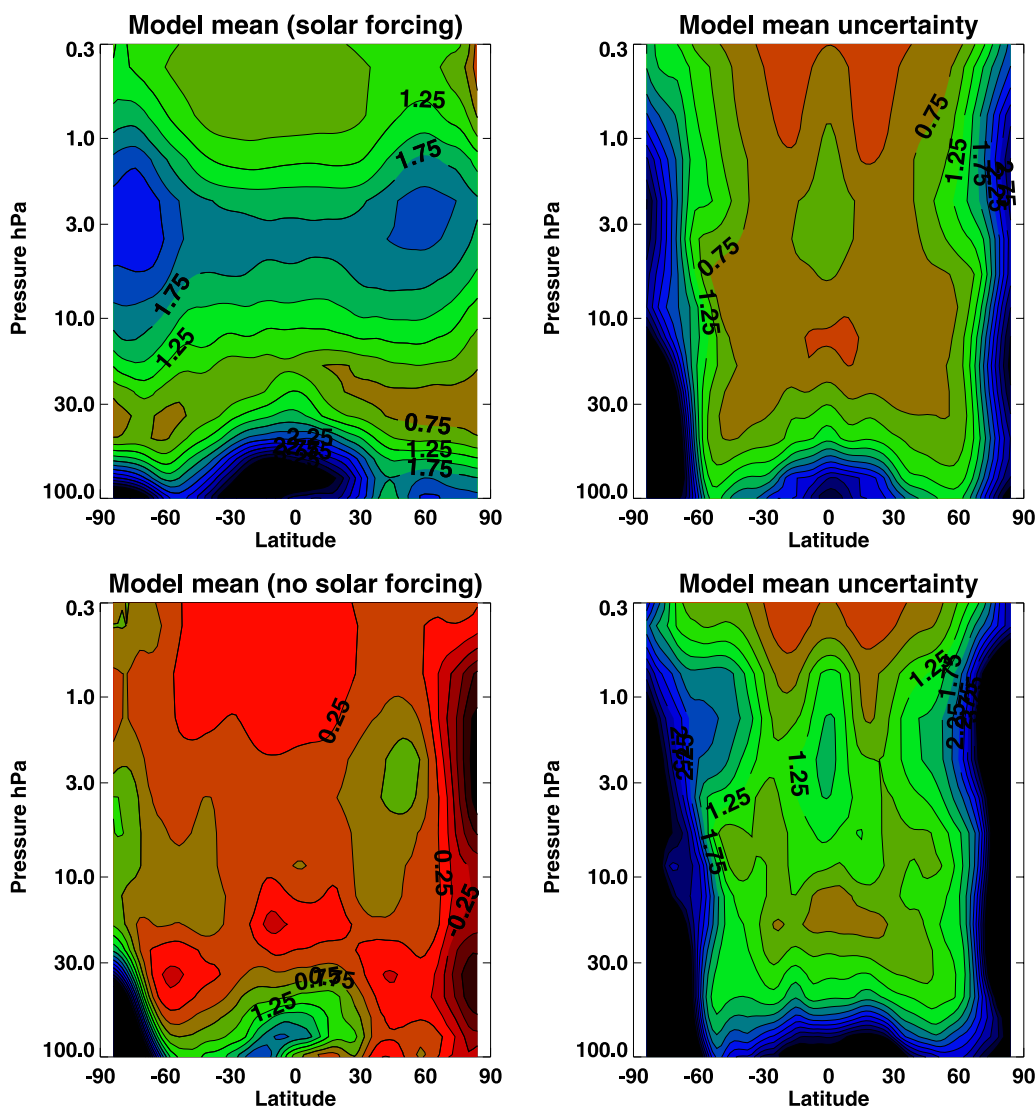


Figure 3. As in Figures 1 and 2, but composites of all the model results which forced a solar cycle in both the radiative heating and photolysis rates (upper panels) and those without solar forcing (lower panels). The contour interval is 0.25%. The model mean uncertainty was computed from the population statistics as $\sigma = \sqrt{\sum \sigma_i^2 / [n(n-1)]}$ for the 8 models with solar forcing and 4 without. 2σ values are plotted.

level, as indicated by the mean model age of air at that location. Figure 6 shows the recomputed solar sensitivity for AMTRAC, WACCM and CMAM (compare Figure 5). The results were found not to be critically dependent on the time lag assumed.

[23] For the period as a whole, 1960–2003, or for 1982–2003, the results have not changed significantly in any of the models at any level in the atmosphere. However, for the period 1960–1981, the results have changed substantially. Indeed, for AMTRAC there is now no significant sensitivity to the period analyzed, at any level. WACCM and CMAM still indicate some sensitivity to the period, although this is somewhat reduced compared with Figure 5 and in any case is similar to the likely uncertainty.

[24] Further analysis shows that for the period 1960–1981 there was a higher correlation between $F_{10.7}$ and SSTs (correlation coefficient 0.38) than either the whole period

1960–2003 (correlation coefficient 0.28), or the period 1982–2003 (correlation coefficient -0.11). Therefore it would appear that the marked difference in solar sensitivities in the different periods is largely due to an aliasing effect between the solar and SST terms. The model results in this paper are mostly from 1980 onwards, and so the aliasing effect would generally be small. In the case of CMAM, the solar cycle is not explicitly included and hence the derived solar response appears as a false solar signal due to the aliasing, especially for the period 1960–1981.

4.4. Solar Cycle in Total Ozone

[25] Figure 7 shows the time series of the globally averaged total ozone for the model simulations, after removing the non-solar terms. For those models which had explicit solar forcing (top and middle panels of Figure 7), a well defined solar cycle is present. For those

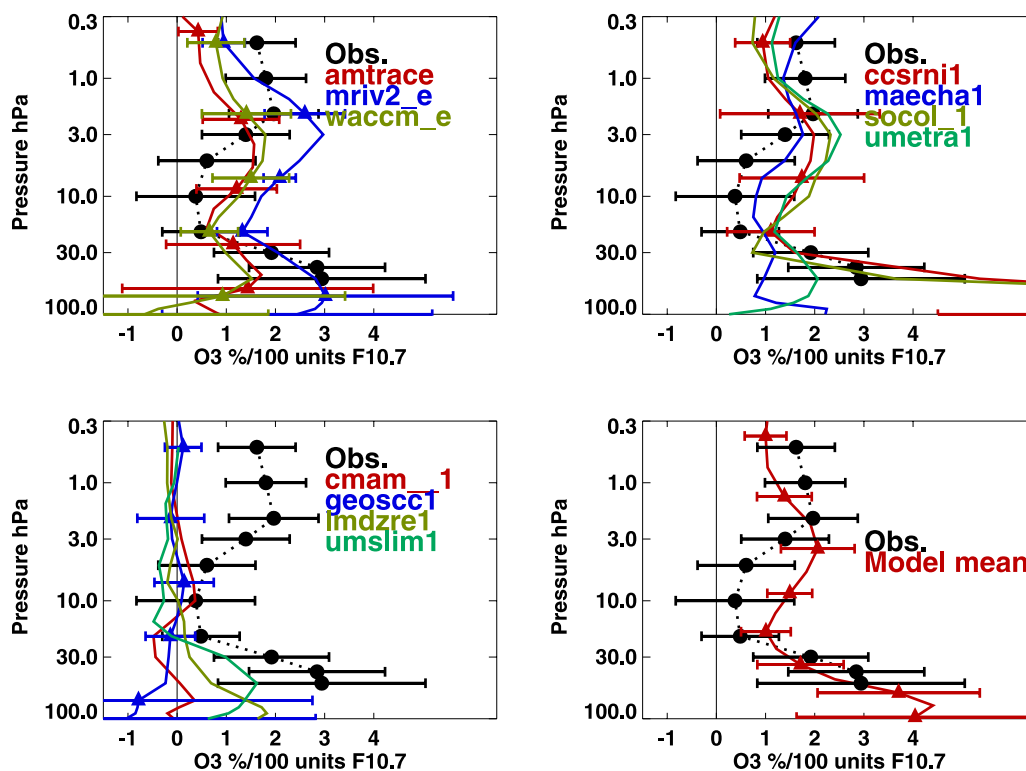


Figure 4. Ozone solar response averaged over the latitude range 25°S to 25°N . The top left panel illustrates the results for ensemble simulations and the top right panel shows the single simulation results, in both cases for models with a solar cycle. The lower left panel illustrates the results for those models without explicit solar forcing. The lower right panel shows a simple mean of the simulations of the models with solar forcing (red line). The dotted black line in all the panels is the mean of the observations from three independent satellite instruments presented by *Soukharev and Hood* [2006]; see text. All the uncertainty ranges are 95% confidence intervals.

models which completed several realizations (Figure 7, upper panel) the solar variability is clearest, especially for AMTRAC and WACCM. In comparison, for those models which completed a single realization (Figure 7, middle panel) the deviations from the solar cycle are typically larger. Note that for the first few years of the AMTRAC simulation, the total ozone was still evolving rapidly away from the initial conditions and the connection with the solar cycle was not clear. The differences between AMTRAC and WACCM in the early part of the record may also be related to the different aerosol distributions used, as this would tend to have more impact in the lower stratosphere.

[26] For the models with no explicit solar forcing, the total ozone deviation time series (Figure 7, lower panel) are very similar in all four models. The results show no clear solar signal, although all the models reveal an oscillation with a 30 year period.

5. Comparison Between Model Results and Measurements for the Ozone Solar Cycle

[27] The most comprehensive database of ozone measurements, supplying both column amounts and vertical distribution, is provided by satellite data (Solar Backscattered Ultraviolet (SBUV); Stratospheric Aerosol and Gas Experiment (SAGE) and the Halogen Occultation Experiment (HALOE)) which have been investigated in detail for solar

effects by *Soukharev and Hood* [2006, and references therein; see also *Randel and Wu*, 2007]. Total ozone from ground-based observations are also considered, updated from *Fioletov et al.* [2002], and supplied courtesy of V. Fioletov. Here the modeled vertical ozone solar sensitivity is compared with the satellite data, and the total column sensitivity is compared with the ground-based observations.

5.1. Solar Sensitivity of the Ozone Vertical Variation

[28] As indicated by *Soukharev and Hood* [2006] the satellite data have large uncertainties locally, especially in high latitudes. Hence in this section we consider only the low latitudes and reduce the random error further by averaging over the latitude range 25°S to 25°N . Also shown in Figure 4 is the observed ozone response, taken from the satellite data presented by *Soukharev and Hood* [2006]. To obtain these values, the mean response was determined for the three individual satellite instruments without regard to the period of the analysis. On account of the different vertical resolutions in the satellite instruments, the lower stratospheric minimum has become spread over a larger range of altitudes than in the individual instruments, but this is accommodated in the uncertainty ranges shown. Also, because of the different periods used to form the observational signal, the mean profile should be considered only representative but a more rigorous analysis is beyond the scope of the current work. As noted in section 4.2, the

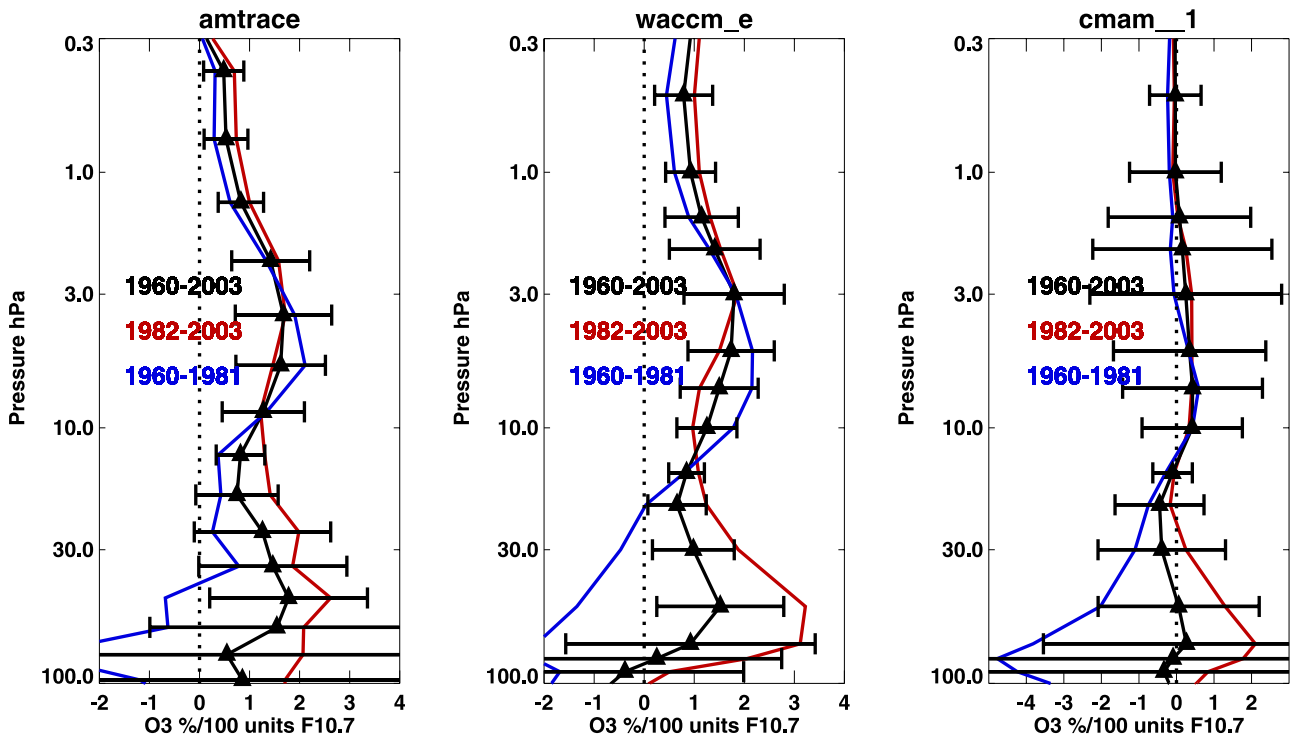


Figure 5. Ozone solar response averaged over the latitude range 25°S to 25°N in AMTRAC, WACCM and CMAM, separated into different periods as indicated. Note the different scaling on the abscissa for CMAM compared with the other two models.

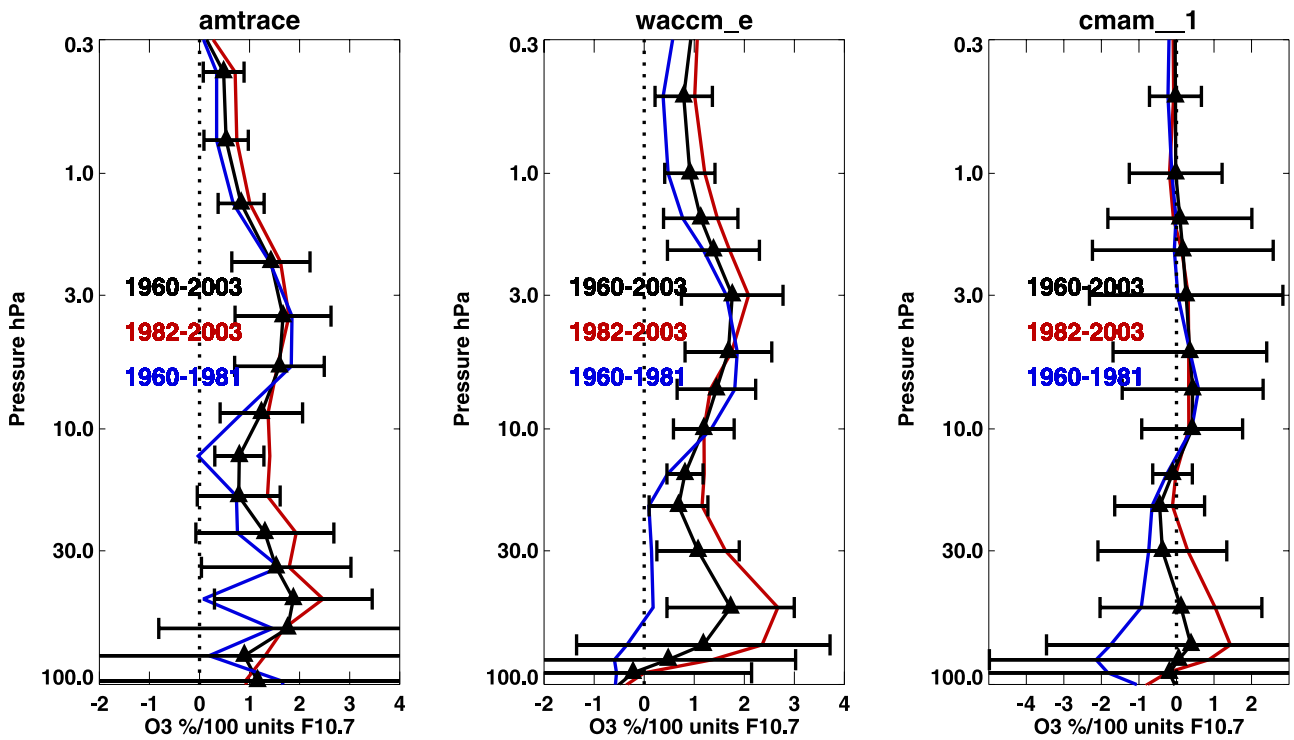


Figure 6. Ozone solar response averaged over the latitude range 25°S to 25°N in AMTRAC, WACCM and CMAM, separated into different periods. In these calculations, SSTs are included as an independent variable in the regression equation. Note the different scaling on the abscissa for CMAM compared with the other two models.

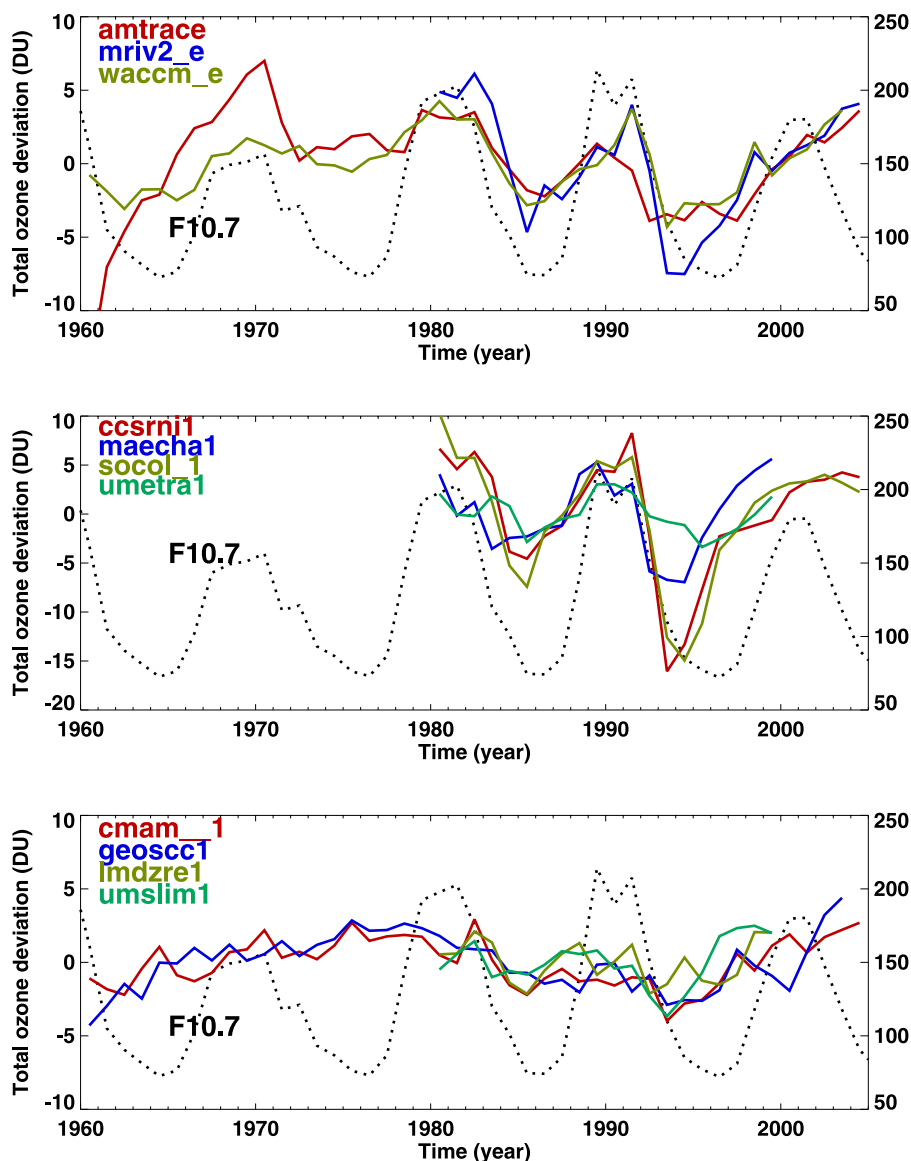


Figure 7. Model simulated globally averaged total ozone with the column mean, aerosol, trend and wind terms removed using the regression equation. The $F_{10.7}$ values are indicated by the broken black line. (top) Mean results for ensemble simulations. (middle) Simulations for single realizations. (bottom) Results for models without solar forcing.

models with solar forcing generally agree well with the observations throughout most of the pressure range indicated. The model results are strictly zonal average values, which is an average over local time, whereas the observations are typically made at fixed local times. Therefore, in the mesosphere, where the diurnal variation of ozone is large, some of the differences between model results and observations may have arisen from a diurnal variation in the actual solar response.

5.2. Solar Sensitivity of the Total Ozone Column

[29] The solar response in total ozone is shown in Figure 8 for the ground-based observations from 1964 onwards, and the full temporal range in each of the model simulations. The results shown here are similar to the ground based results shown by *Randel and Wu* [2007], although they

show their results in DU rather than %. Also, the use of different proxies in the regression analysis as well as different periods lead to some differences in the solar signal obtained. More importantly, *Randel and Wu* indicate that the solar signal obtained from satellite data is much higher than from the ground-based data, although the difference is in most cases not statistically significant.

[30] In both observations and model simulations, the solar response is about 1–2% of the annual mean per 100 units of the $F_{10.7}$ flux. In the tropics, where the errors are smallest, the response is statistically significant for most of the models (error bars not shown) and the average model response is well within the 95% confidence range of the observations. Away from the tropics the errors are larger and there are large differences between the models, especially in the Southern Hemisphere polewards of 60S. As in the case

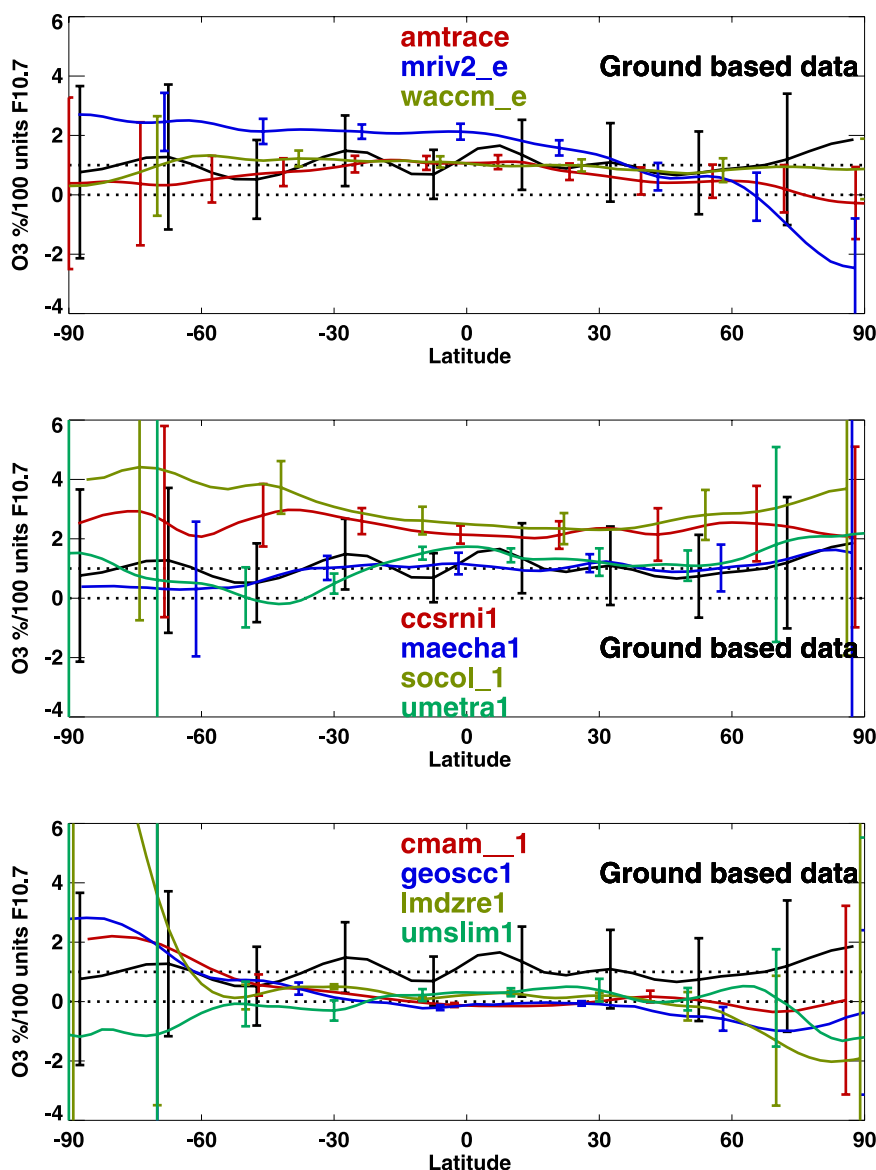


Figure 8. Total ozone solar response in % per 100 units of $F_{10.7}$ simulated by the models as a function of latitude in comparison with observations. The 95% confidence intervals for the observations is indicated at every other grid point. (top) Mean results for those models which completed ensembles. (middle) Model results for single simulation runs. (bottom) Results for those models without explicit solar forcing. The broken black lines indicate solar responses of 0% and 1%.

of the vertical ozone response, this may be attributed to the interannual variability of the different models. Similar results were also found for those models which ran ensembles, and there is less spread between the individual model results. For both AMTRAC and WACCM the solar response closely followed the observations, especially in middle and low latitudes. In the polar regions the MRI ensemble mean results diverged from the other ensemble results although all the uncertainties are large in high latitudes.

[31] Of the models without explicit solar forcing the solar response was close to zero, except in the polar regions. Over the Arctic, the uncertainties were generally large but the model solar responses were not significantly different from zero. Over Antarctica LMDZrepro showed a statistically

significant response reflecting the aliasing to the aerosol term discussed in section 4.1.

6. Results: Temperature

[32] The simulated latitude and pressure variations of the solar response for all the models are shown in Figures 9 and 10, arranged according to simulation attributes as for the ozone plots, Figures 1 and 2. As in the case of the ozone simulations, the signal in those models without explicit solar forcing was generally negligible (Figure 10). The exceptions to this may have been due to the short length of the simulations, or possibly some aliasing with the ozone hole development as was suggested in the case of LMDZrepro for ozone (compare Figure 10 with Figure 2). As in the case

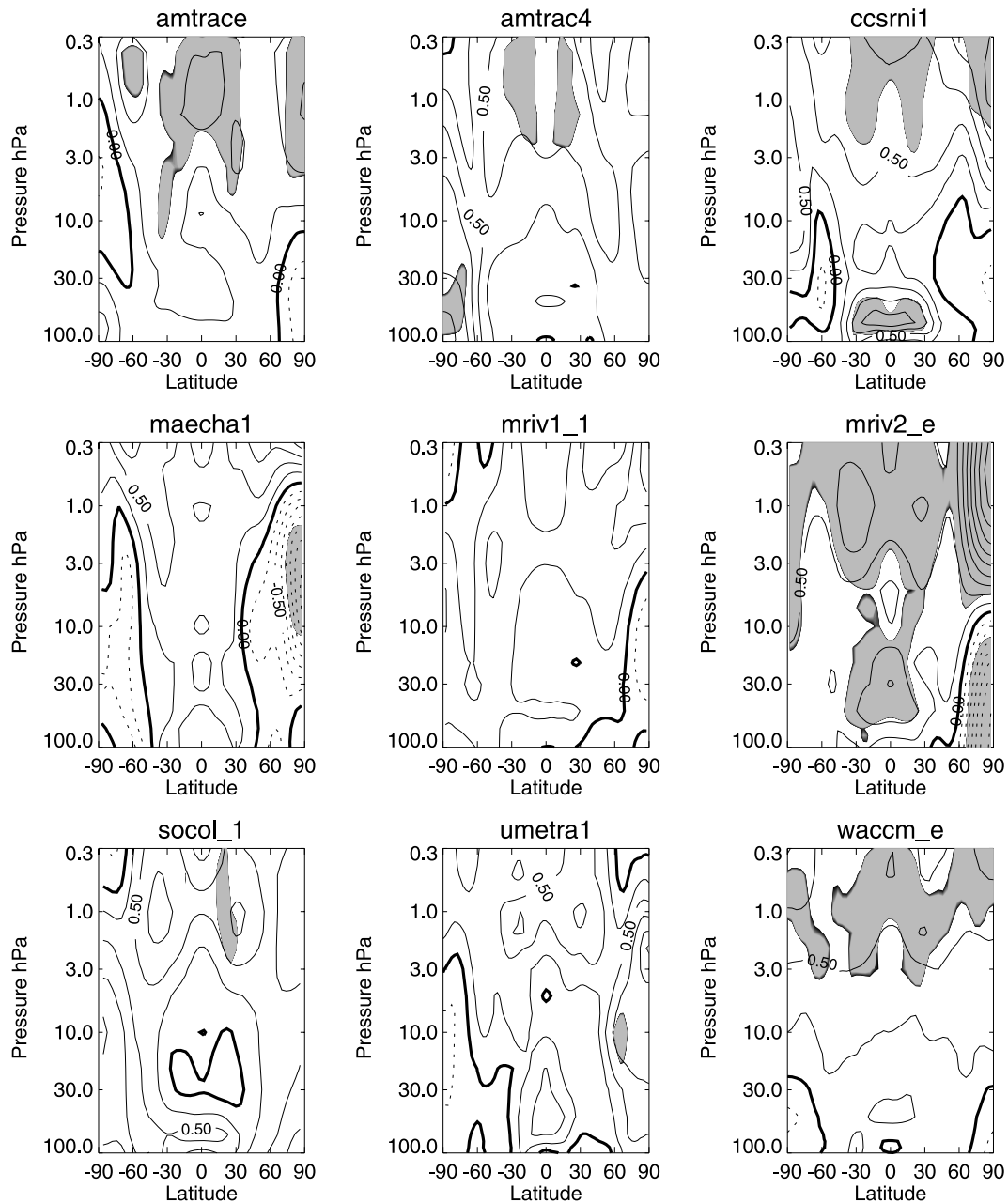


Figure 9. Annually averaged temperature solar cycle response (K per 100 units $F_{10.7}$), as a function of latitude and pressure, for those models which explicitly included solar forcing. The contour interval is 0.25 and negative values are drawn with broken contours. The zero contour is drawn bold. The shaded region indicates where the solar response is significantly different from zero at the 95% confidence level.

of ozone, the temperature response in the individual models with solar forcing (Figure 9) differs in detail, but many of the model analyses suffer from the short integration time (only two cycles in most cases). For those models which completed ensemble runs, the solar response varied between the individual members but this was not statistically significant. Single simulations of 4 or 5 solar cycles are not sufficient to establish a reliable solar signal. For the ensemble runs the domain over which the solar signal is statistically significant is in the upper stratosphere. The peak temperature response is similar in WACCM and AMTRAC, but much larger in MRI, consistent with the ozone differ-

ences. Comparison between MRI version 1 (MRIV1) and version 2 (MRIV2) indicates the impact of the photolysis rates which increased the solar temperature response especially in the polar upper stratosphere. The temperature solar cycle response of MRIV1 in the tropics is very similar to that due to UV heating alone under the fixed dynamical heating assumption [Shibata and Kodera, 2005].

[33] The mean of the model results is shown in Figure 11 separated into those simulations which included a solar cycle and those which did not. As in the case of ozone, for the solar forced runs, the mean response was approximately independent of latitude from 60S to 60N in the

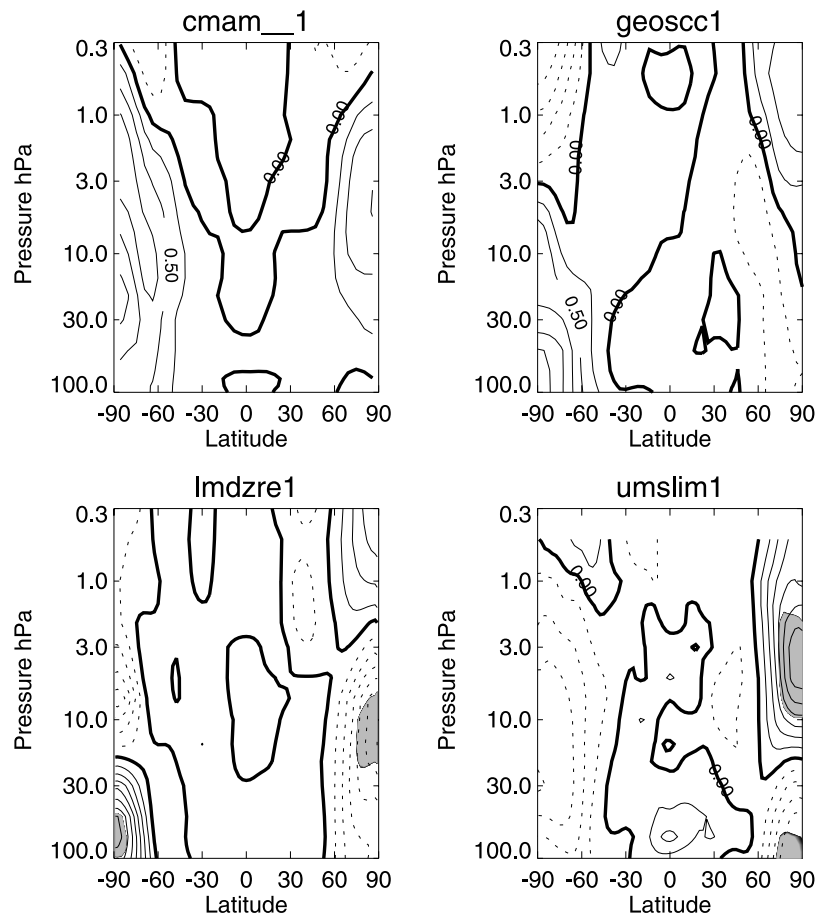


Figure 10. Annually averaged temperature solar cycle response (K per 100 units $F_{10.7}$), as a function of latitude and pressure, for those models which did not explicitly include solar forcing.

middle and upper stratosphere. In the tropics a double peak structure is present, although the lower stratospheric maximum is not statistically significant. There were fewer simulations which did not have a solar cycle and therefore the uncertainty of the model mean is larger by about a factor of two (Figure 11, bottom right). The derived solar response is substantially smaller than for the solar forced runs, and is nowhere statistically significant.

[34] The results for the low latitude average are shown in Figure 12. Given typical uncertainty ranges (2σ) of ± 0.2 K/100 units $F_{10.7}$, the results are generally in agreement with each other throughout the pressure range. In addition, those models without explicit solar forcing (Figure 12, lower left) are consistent with zero temperature solar response. The results of Figure 12 are also similar to the ozone response shown in Figure 4, with a double maximum feature, although it is weaker than in ozone and not statistically significant. This is discussed further in section 8. In Figure 12, observed values derived from the data of *Scaife et al.* [2000] are indicated by the dotted black line. In the model mean (Figure 12, lower right), the model results agree with observations taking account of the uncertainties in model and observations, although the model results are typically at the lower end of the observed range.

[35] Although temperature measurements have a longer history than ozone measurements, to obtain an accurate solar signal requires very careful analysis of data that have been specially processed to eliminate data discontinuities due to the change in observing systems. The only consistent data source throughout the stratosphere are specially processed data from the Stratospheric Sounding Unit (SSU) and Microwave Sounding Unit (MSU). Data that have undergone suitable screening have been presented by *Scaife et al.* [2000] as well as *Randel et al.* (personal communication, 2007). Recently, the SSU data have been further corrected for the overall trend in CO_2 amounts [*Shine et al.*, 2008]. Although this affects the temperature trend determined from the SSU data, we here assume that the solar signal has not been significantly affected. Other analyses using data assimilations [e.g., *Crooks and Gray*, 2005] are not clearly superior as they would also not have taken into account the recent corrections of *Shine et al.* [2008]. Data in the very low stratosphere are also available from radiosondes which have also been suitably screened for accuracy (*Randel et al.*, personal communication, 2007). The satellite data have a broad maximum in solar response peaking at the equator in the middle to upper stratosphere. A slight reduction in temperature solar response is suggested

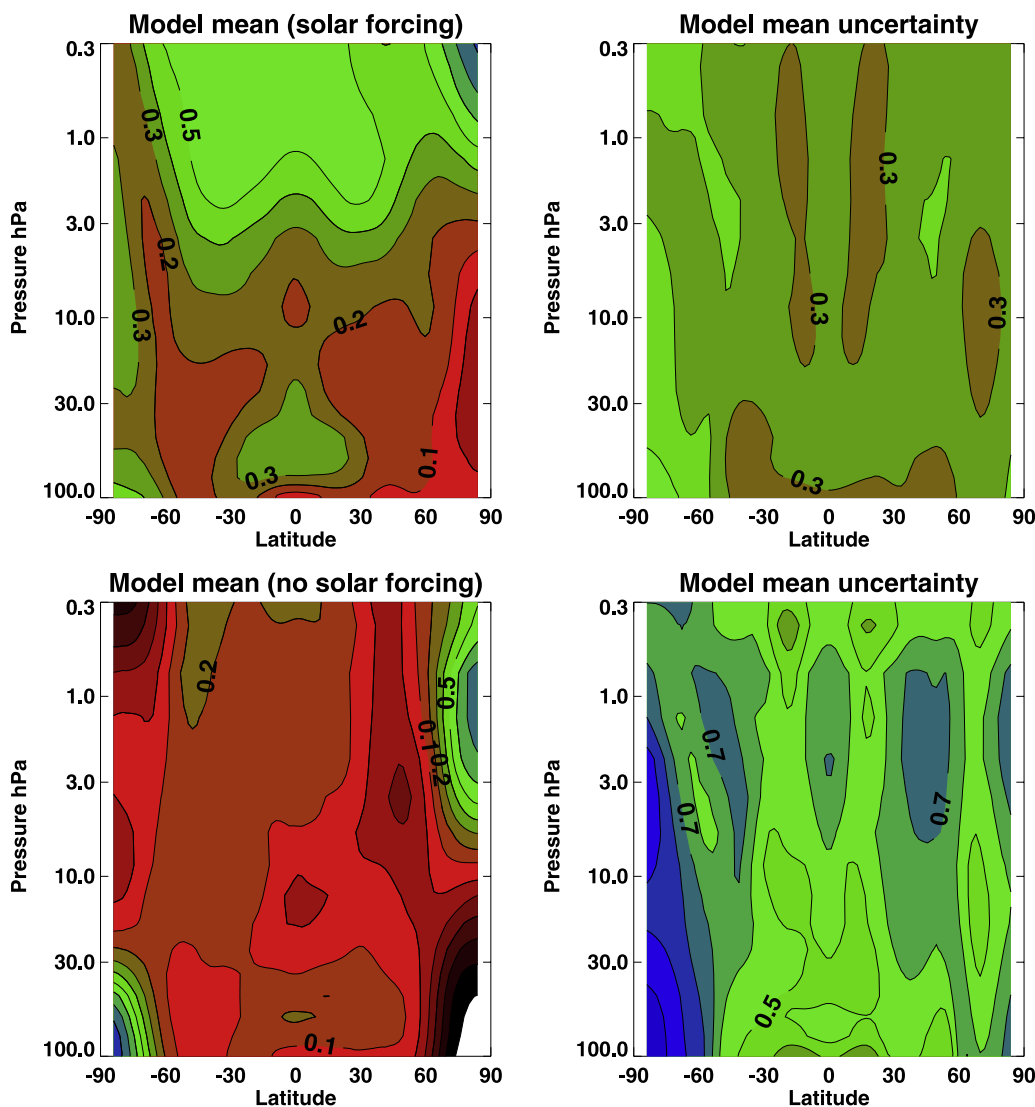


Figure 11. As in Figures 9 and 10, but composites of all the model results which forced a solar cycle in both the radiative heating and photolysis rates (upper panels) and those without solar forcing (lower panels). The contour interval is 0.1 K. The model mean uncertainty was computed from the population statistics as $\sigma = \sqrt{\sum \sigma_i^2 / [n(n-1)]}$ for the 8 models with solar forcing and 4 without. 2σ values are plotted.

in the radiosonde data near 20 hPa, which also appears in the assimilated data presented by *Crooks and Gray* [2005]. The satellite data have too low a vertical resolution to reveal this feature which in any case is not statistically significant in the analysis of *Randel et al.* (personal communication, 2007).

7. Diagnosis of Lower Stratospheric Transport

[36] Direct measures of transport in coupled chemistry climate models are difficult to obtain. Here, we analyze briefly water vapor and age of air for solar cycle signals. Above the hygropause, water vapor is an approximately conserved tracer. The vertical gradient is positive with height due to methane oxidation which has a longer timescale than the advective time scale. A reduction during high solar flux implies enhanced upward motion at this time

due to the transport of lower values from below. Some change in water at the hygropause is also expected from freeze drying. Assuming that processes are reasonably linear, the solar cycle response in temperature at the hygropause (at about 70 hPa) is positive and about 0.2 K in most models. This should give rise to a positive water vapor solar response, assuming no change in transport, of about 3% due to an increase in the saturated vapor pressure.

[37] Age of air is a time integrated quantity which in AMTRAC was shown to be inversely related to the tropical upwelling [*Austin and Li*, 2006] over multi-decadal time scales. However, in AMTRAC the tropical upwelling did not display a solar cycle dependence [*Austin et al.*, 2007a]. Assuming a fixed tropical pipe for entry into the stratosphere, the difference in the age of air between mid-latitudes and the tropics should also be inversely proportional to vertical velocity [*Neu and Plumb*, 1999]. While it cannot be

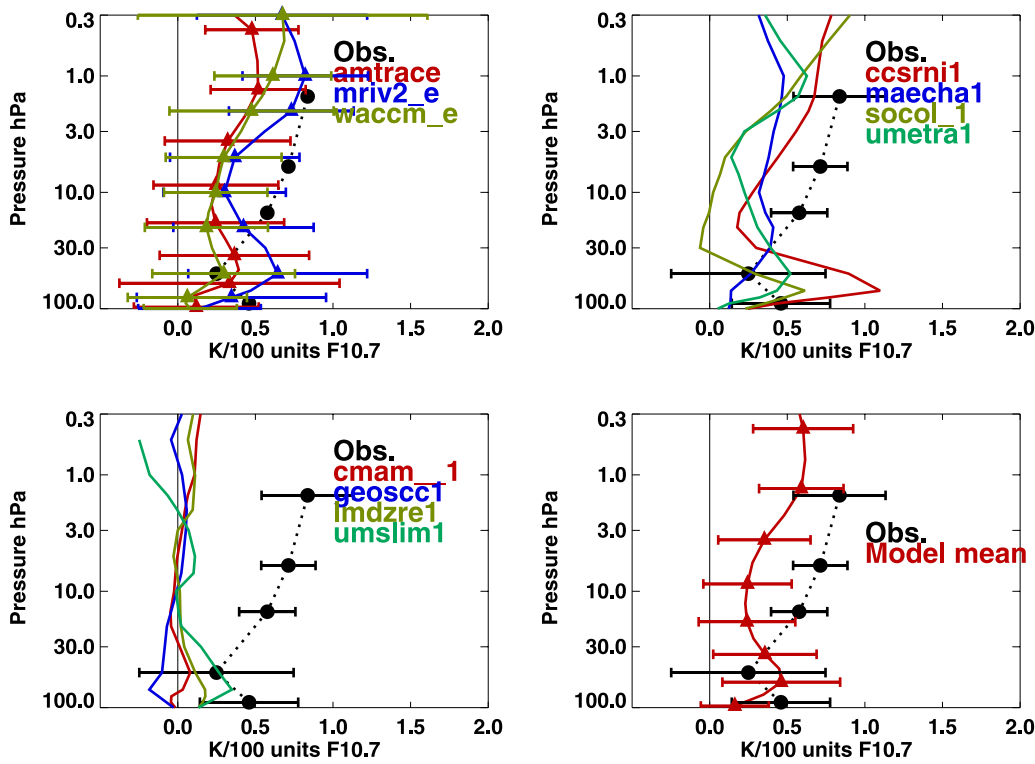


Figure 12. Temperature solar response averaged over the latitude range 25°S to 25°N. The upper left panel are the results from ensemble simulations and the upper right panel are the results from single simulations, in both cases for models with a solar cycle. The lower left panel illustrates the results for those models without explicit solar forcing. The lower right panel shows the mean of all the models with explicit solar forcing. The solar cycle derived from SSU and MSU data is indicated by the dotted black line, and data are reprocessed from *Scaife et al.* [2000].

shown here that age of air and vertical velocity are strictly in inverse proportion to each other, *Neu and Plumb* [1999] and *Austin and Li* [2006] show that the two quantities are clearly closely related.

[38] Concentrating on the low latitude region where the solar cycle in many quantities is more robust, Figure 13 shows the model results for water vapor. For those models without explicit solar forcing, the water vapor signal is not

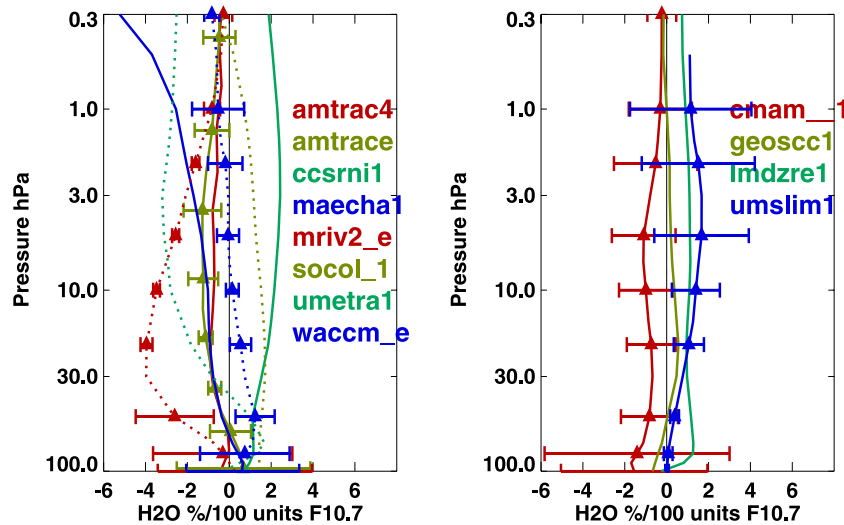


Figure 13. Water vapor solar response averaged over the latitude range 25°S to 25°N in those models with a solar cycle (left), and in those models without explicit solar forcing (right). Models are arranged in alphabetic order in each panel, and the line colors cycle through red–brown–green–blue. The first 4 models are given by solid lines and the second four by dotted lines.

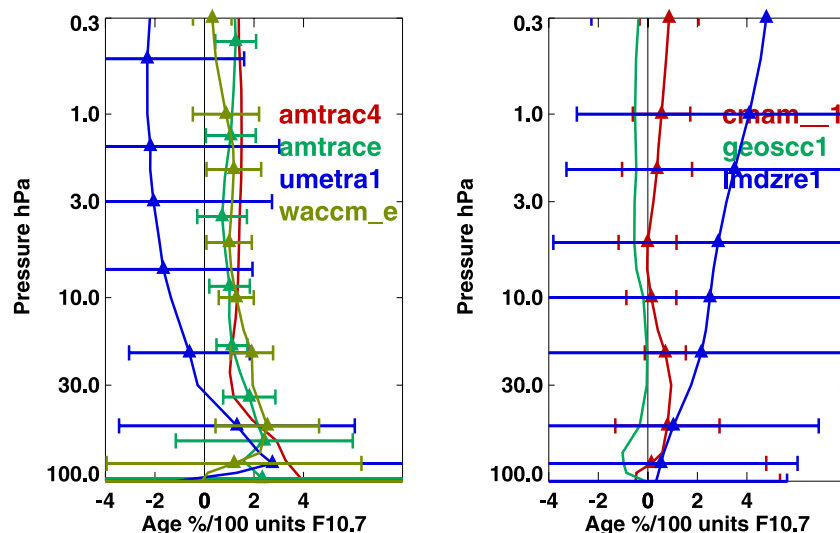


Figure 14. Age of air solar response averaged over the latitude range 25°S to 25°N in those models with a solar cycle (left), and in those models without explicit solar forcing (right). For clarity, the error bars are not shown for all the models.

statistically significant (Figure 13, right). For the models with explicit solar forcing (Figure 13, left), the derived water vapor signal is much larger. Although there is no consensus between the models in the overall change in water vapor amounts, after allowance for the change in temperature at the hygropause indicated above, most of the results would imply a decrease in water vapor. Hence by the arguments above an effective increase in the upwelling is simulated for higher solar fluxes.

[39] Of the models included here, only a small number diagnosed age and the results for the low latitudes are shown in Figure 14. The LMDZrepro model simulated a larger signal than the other models but because of the short integration time the uncertainties are large and the results are not statistically significant. The other two models without explicit solar forcing revealed a small response in the age of air, similar to the other diagnostics previously presented. Of those models which included a solar cycle, two indicated a correlation between the solar cycle and age, while the other showed an anticorrelation. For the ensemble averages shown in Figure 14 a typical solar response is 1% per 100 units of $F_{10.7}$, and this is just statistically significant at most levels above 50 hPa. Although the age of air results for UMETRAC are not statistically significant, they are consistent with the water vapor results in Figure 13.

[40] As with a number of diagnostics presented in this paper, although the individual ensemble members often vary substantially in their solar response, the AMTRAC and WACCM ensemble means agree well with each other. The increase in the age of air in these models for high solar flux appears to be inconsistent with the water vapor results (after correcting for the temperature effect) and imply decreased upward motion during high solar flux.

8. Discussion on the Structure of the Tropical Ozone Response

[41] The current paper has confirmed the major progress which has taken place in simulating the solar cycle in ozone.

Compared with the previous situation in which model results agreed poorly with observations [Soukharev and Hood, 2006], agreement is now obtained within the error bars of the observations and models concerning the structure of the tropical ozone solar response. Earlier work [e.g., Callis et al., 2001; Langematz et al., 2005] has tended to explain the inability to simulate the observed minimum by including an additional chemical loss due to energetic electron precipitation, although it is not supported by experiments with a more realistic description of this odd nitrogen source [Rozanov et al., 2005a]. The results obtained here and elsewhere [Kodera and Kuroda, 2002; Schmidt and Brasseur, 2006] now support more the idea that the structure is better described as a "double vertical peak" with the upper peak due to photolysis and the lower peak due to transport. Between these two regions, neither process is particularly sensitive to the solar cycle. Further, in the mean model result shown in Figure 3, the minimum solar response broadly follows the tropopause, with a higher altitude over the tropics and a lower altitude over the polar regions. The CMAM results (Figures 5 and 6) also provide indirect evidence of the importance of dynamics on the lower stratospheric solar response. For this model, a solar response occurred despite the absence of explicit solar forcing, but this response varied according to the period. In this case, it is plausible that this is a dynamical effect induced by the sea surface temperatures which bear a different relationship to $F_{10.7}$ during different periods.

[42] The Kodera and Kuroda [2002] study used a simplified model to show that for the winter season, solar forcing should result in a decrease in the upward motion. If it is assumed that the winter season dominates the annual average, then this would give rise to the temperature and ozone effects seen in the observations and simulations. Examination of the model simulations for transport changes, though, produced ambiguous results for the limited data sets available: the model results for water vapor and age of air were not apparently consistent with each other.

[43] The results obtained in the lower stratosphere were largely independent of whether or not the QBO was present. However, in earlier results in which tropical wind was not included as an independent variable, MAECHAM4/CHEM results did not show a prominent lower stratospheric peak. This suggests that for short simulations the difficulty of separating the QBO signal is leading more to aliasing [Lee and Smith, 2003] than a direct impact. A possible resolution therefore of the apparent contrast between the results here and those published [e.g., McCormack, 2003] is that most of the simulations are now long enough for the statistical impact of the solar cycle to be separated from the QBO. Nonetheless it is possible that the QBO is partially contributing to the results for a given model [e.g., McCormack et al., 2007], but that this is a smaller effect than the differences between models.

[44] In results shown here, the ozone solar response was also found to be relatively insensitive to period, once the aliasing of the SSTs with the solar cycle during the years 1960–1981 was considered. Aside from this complication of the correlation between the SSTs and the solar cycle, by using the observed SSTs instead of climatological values the models might be expected to simulate improved, stronger tropospheric wave forcing which is no longer smoothed as much over time. The Brewer-Dobson circulation is then more realistic, resulting in an improvement in the simulated sensitivity to the solar cycle of ozone transport. This would imply the need for observed SSTs and a fully varying solar phase, as have been incorporated in the model simulations here. Support for these arguments comes from additional simulations of models used here [Austin et al., 2007a; Marsh et al., 2007] as well as the many simulations shown by Soukharev and Hood [2006] in which the lower stratospheric tropical maximum response is not well reproduced with climatological SSTs and fixed phase solar forcing.

[45] It would be natural to conclude that the correct details of the forcings are needed to obtain the correct lower stratospheric transport, and hence to simulate the secondary lower stratospheric ozone peak response. However, recently other models have been able to simulate this feature using climatological SSTs and fixed solar forcing (maximum/minimum) [Schmidt and Brasseur, 2006; T. Nagashima, personal communication, 2007]. A pertinent question would be whether those models produce a stronger double peak structure when the observed forcings are used.

9. Summary and Conclusion

[46] Multi-decadal simulations of coupled chemistry climate models have been analyzed for the presence of the solar cycle in ozone and temperature, and compared with satellite measurements. The simulations are from those described by Eyring et al. [2006] and have observed forcings (sea surface temperatures - SSTs, aerosol and solar cycle) for the period 1950 to 2005, or a subset thereof, although Eyring et al. [2006] did not analyze the results for the solar cycle. As a function of latitude and pressure, the derived solar signals in the models were very variable from point to point and subject to large uncertainty. Therefore much of the analysis concentrated on the tropical average response for which smaller model and observation uncertainties could be established. In addition, several models

performed ensemble runs which helped to reduce further the uncertainty in the solar signal.

[47] The model results for ozone generally agreed with observations averaged over the latitude range 25°S to 25°N, and indicate a peak solar response of about 2% per 100 units of 10.7cm radio flux. Given typical solar minimum to solar maximum change in flux of about 125 units, this implies a response of about 2.5% from solar minimum to maximum. The results are an improvement over, for example, the compendium of model results presented by Soukharev and Hood [2006]. In particular, all the models presented here which forced a solar cycle reproduce a double maximum solar response in the stratosphere, and further investigations were carried out to try to determine its cause.

[48] Some of the model simulations had a quasi-biennial oscillation (QBO), either naturally occurring or forced from observations, but other models did not. The results obtained, particularly regarding the presence of the tropical ozone minimum solar response were largely independent of whether or not the QBO was present.

[49] In the two longest simulations, both models were consistent with each other and the results were initially found to be substantially different for the first two solar cycles (1960–1981) than the last two solar cycles (1982–2003). The differences in the two periods were small in the middle and upper stratosphere, but in the lower stratosphere, the ozone response was negative for 1960 to 1981 and positive for 1982 to 2003. Moreover, the latter results were consistent with the solar sensitivity derived from satellite data over approximately the same period. Further analysis showed that when an additional term representing sea surface temperatures was included in the regression much of the sensitivity to period disappeared but for the results over the whole period of simulations, the results did not change significantly. This suggests that aliasing between the SSTs and solar flux artificially affected the results over the period 1960–1981. The analysis of total ozone from the model results also revealed a solar signal which in most cases was in agreement with that derived from observations. The signal was found to be small in middle latitudes, about 1.5% from solar minimum to solar maximum, and statistically significant. The signal only became large in high latitudes where the uncertainty was even larger, so that the signal could not be distinguished from a zero response.

[50] The temperature solar response in the models was found to peak in the upper stratosphere at about 0.6 K per 100 units of 10.7 cm radio flux, slightly smaller than the observed value of 0.8 K, derived from the data of Scaife et al. [2000]. The temperature and ozone responses are correlated in accordance with previous modeling studies [e.g., Labitzke et al., 2002, Rozanov et al., 2005c]. In the upper stratosphere, additional ozone leads to additional solar heating, while in the lower stratosphere reduced upward motion induces both reduced adiabatic cooling and less transport of low ozone amounts. The observed temperature solar signal is subject to large uncertainty due to the change in instrumentation over the satellite period. Also, the satellite data have low vertical resolution. It is unclear therefore whether there is a minimum in the temperature solar response in the lower or middle stratosphere, which would be needed for the hypothesis regarding transport influences, discussed in section 8, to be confirmed.

[51] The age of air results were ambiguous, although two of the models which completed ensemble runs tend to support the Kodera and Kuroda argument of decreased upward motion during high solar forcing. The inconsistencies between models and between different transport measures need to be resolved by completing more simulations of the complete cycle with a larger suite of models, including age as a diagnostic. Another possibility is to investigate the model results of generalized Lagrangian mean vertical velocity or the tropical upwelling. However, this has not been explored because of the large interannual variability which for example was too large in AMTRAC to detect a solar cycle in tropical upwelling [Austin et al., 2007a]. Moreover the improved performance of current models emphasizes the need to obtain improved observational analyses of the solar cycle for accurate model validation.

[52] **Acknowledgments.** The satellite ozone solar cycle data were kindly supplied by B. Soukharev and the ground based data were kindly supplied by V. Fioletov. JA's research was administered by the University Corporation for Atmospheric Research at the NOAA Geophysical Fluid Dynamics Laboratory, CSRNIES research was supported by the Global Environmental Research Fund of the Ministry of the Environment of Japan (A-071). The MPI-M, MPI-C and INGV acknowledge support of the SCOUT-O3 Integrated Project which is funded by the European Commission. Katja Matthes is supported by a Marie Curie Outgoing International Fellowship within the 6th European Community Framework Programme. We thank the Reviewers for their helpful comments on the material.

References

- Akiyoshi, H., T. Sugita, H. Kanzawa, and N. Kawamoto (2004), Ozone perturbations in the Arctic summer lower stratosphere as a reflection of NO_x chemistry and planetary scale wave activity, *J. Geophys. Res.*, *109*, D03304, doi:10.1029/2003JD003632.
- Austin, J., and N. Butchart (2003), Coupled chemistry-climate model simulations for the period 1980 to 2020: ozone depletion and the start of ozone recovery, *Q.J.R. Meteorol. Soc.*, *129*, 3225–3249.
- Austin, J., and F. Li (2006), On the relationship between the strength of the Brewer-Dobson circulation and the age of stratospheric air, *Geophys. Res. Lett.*, *33*, L17807, doi:10.1029/2006GL026867.
- Austin, J., and R. J. Wilson (2006), Ensemble simulations of the decline and recovery of stratospheric ozone, *J. Geophys. Res.*, *111*, D16314, doi:10.1029/2005JD006907.
- Austin, J., L. L. Hood, and B. E. Soukharev (2007a), Solar cycle variations of stratospheric ozone and temperature in simulations of a coupled chemistry-climate model, *Atmos. Chem. Phys.*, *7*, 1693–1706.
- Austin, J., R. J. Wilson, F. Li, and H. Vömel (2007b), Evolution of water vapor concentrations and stratospheric age of air in coupled chemistry-climate model simulations, *J. Atmos. Sci.*, *64*, 905–921.
- Beagley, S. R., J. de Grandpré, J. N. Koshyk, N. A. McFarlane, and T. G. Shepherd (1997), Radiative-dynamical climatology of the first generation Canadian Middle Atmosphere Model, *Atmos. Ocean*, *35*, 293–331.
- Bengtsson, L., K. I. Hodges, E. Roeckner, and R. Brokopf (2006), On the natural variability of the pre-industrial European climate, *Clim. Dyn.*, *27*, 743–760, doi:10.1007/s00382-006-0168-y.
- Bloom, S., et al. (2005), Documentation and validation of the Goddard Earth Observing System (GEOS) data assimilation system - Version 4, in *Global Modeling Data Assimilation 104606*, Tech. Rep. Ser. 26, NASA Goddard Space Flight Cent., Greenbelt, Md.
- Brasseur, G., and S. Solomon (1987), *Aeronomy of the Middle Atmosphere*, D. Reidel, Dordrecht, Netherlands.
- Callis, L. B., M. Natarajan, and J. D. Lambeth (2001), Solar-atmosphere coupling by electrons (SOLACE): 3. Comparisons of simulations and observations, 1979–1997, issues and implications, *J. Geophys. Res.*, *106*, 7523–7539.
- Crooks, S. A., and L. J. Gray (2005), Characterization of the 11-year solar signal using multiple regression analysis of the ERA-40 dataset, *J. Clim.*, *18*, 996–1015.
- de Grandpré, J., S. R. Beagley, V. I. Fomichev, E. Griffioen, J. C. McConnell, A. S. Medvedev, and T. G. Shepherd (2000), Ozone climatology using interactive chemistry: Results from the Canadian Middle Atmosphere Model, *J. Geophys. Res.*, *105*, 26,475–26,492.
- Egorova, T., E. Rozanov, E. Manzini, M. Haberreiter, W. Schmutz, V. Zubov, and T. Peter (2004), Chemical and dynamical response to the 11-year variability of the solar irradiance simulated with a chemistry-climate model, *Geophys. Res. Lett.*, *31*, L06119, doi:10.1029/2003GL019294.
- Egorova, T., E. Rozanov, V. Zubov, E. Manzini, W. Schmutz, and T. Peter (2005), Chemistry-climate model SOCOL: A validation of the present-day climatology, *Atmos. Chem. Phys.*, *5*, 1557–1576.
- Eyring, V., et al. (2006), Assessment of temperature, trace species and ozone in chemistry-climate model simulations of the recent past, *J. Geophys. Res.*, *111*, D22308, doi:10.1029/2006JD007327.
- Fioletov, V. E., G. E. Bodeker, A. J. Miller, R. D. McPeters, and R. Stolarski (2002), Global and zonal total ozone variations estimated from ground-based and satellite measurements: 1964–2000, *J. Geophys. Res.*, *107*(D22), 4647, doi:10.1029/2001JD001350.
- Garcia, R. R., D. R. Marsh, D. E. Kinnison, B. A. Boville, and F. Sassi (2007), Simulation of secular trends in the middle atmosphere 1950–2003, *J. Geophys. Res.*, *112*, D09301, doi:10.1029/2006JD007485.
- Haigh, J. D. (1994), The role of stratospheric ozone in modulating the solar radiative forcing of climate, *Nature*, *370*, 544–546.
- Haigh, J. D. (1996), The impact of solar variability on climate, *Science*, *272*, 981–984.
- Haigh, J. D., and M. Blackburn (2006), Solar influences on stratosphere troposphere dynamical coupling, *Space Sci. Rev.*, *125*, 331–344.
- Hood, L. L., and B. E. Soukharev (2006), Solar induced variations of odd nitrogen: Multiple regression analysis of UARS HALOE data, *Geophys. Res. Lett.*, *33*, L22805, doi:10.1029/2006GL028122.
- Kodera, K., and Y. Kuroda (2002), Dynamical response to the solar cycle, *J. Geophys. Res.*, *107*(D24), 4749, doi:10.1029/2002JD002224.
- Krivova, N. A., S. K. Solanki, and L. Floyd (2006), Reconstruction of solar UV irradiance in cycle 23, *Astron. Astrophys.*, *452*, 631–639.
- Labitzke, K., J. Austin, N. Butchart, J. Knight, M. Takahashi, M. Nakamoto, T. Nagashima, J. Haigh, and V. Williams (2002), The global signal of the 11-year solar cycle in the stratosphere: observations and model results, *J. Atmos. Sol. Terr. Phys.*, *64*, 203–210.
- Langematz, U., J. L. Grenfell, K. Matthes, P. Mieth, M. Kunze, B. Steil, and C. Brühl (2005), Chemical effects in 11-year solar cycle simulations with the Freie Universität Berlin Climate Middle Atmosphere Model with online chemistry (FUB-CMAM-CHEM), *Geophys. Res. Lett.*, *32*, L13803, doi:10.1029/2005GL022686.
- Lee, H., and A. K. Smith (2003), Simulation of the combined effects of solar cycle, quasi-biennial oscillation, and volcanic forcing on stratospheric ozone changes in recent decades, *J. Geophys. Res.*, *108*(D2), 4049, doi:10.1029/2001JD001503.
- Lefèvre, F., G. P. Brasseur, I. Folkins, A. K. Smith, and P. Simon (1994), Chemistry of the 1991–92 stratospheric winter: Three dimensional model simulations, *J. Geophys. Res.*, *99*, 8183–8195.
- Lefèvre, F., F. Figarol, K. S. Carslaw, and T. Peter (1998), The 1997 Arctic ozone depletion quantified from three-dimensional model simulations, *Geophys. Res. Lett.*, *25*(13), 2425–2428, doi:10.1029/98GL51812.
- Lott, F., L. Fairhead, F. Hourdin, and P. Levan (2005), The stratospheric version of LMDz: Dynamical Climatologies, Arctic Oscillation, and Impact on the Surface Climate, *Clim. Dyn.*, *25*, 851–868, doi:10.1007/s00382-005-0064-x.
- Manney, G. L., et al. (2008), The evolution of the stratopause during the 2006 major warming: Satellite Data and Assimilated Meteorological Analyses, *J. Geophys. Res.*, doi:10.1029/2007JD009097, in press.
- Manzini, E., B. Steil, C. Brühl, M. A. Georgetta, and K. Krüger (2003), A new interactive chemistry-climate model: 2. Sensitivity of the middle atmosphere to ozone depletion and increase in greenhouse gases and implications for recent stratospheric cooling, *J. Geophys. Res.*, *108*(D14), 4429, doi:10.1029/2002JD002977.
- Marsh, D. R., R. R. Garcia, D. E. Kinnison, B. A. Boville, S. C. Solomon, and K. Matthes (2007), Modeling the whole atmosphere response to solar cycle changes in radiative and geomagnetic forcing, *J. Geophys. Res.*, *112*, D23306, doi:10.1029/2006JD008306.
- Matthes, K., U. Langematz, L. J. Gray, K. Kodera, and K. Labitzke (2004), Improved 11-year solar signal in the Freie Universität Berlin Climate Middle Atmosphere Model (FUB-CMAM), *J. Geophys. Res.*, *109*, D06101, doi:10.1029/2003JD004012.
- Matthes, K., Y. Kuroda, K. Kodera, and U. Langematz (2006), Transfer of the solar signal from the stratosphere to the troposphere: Northern winter, *J. Geophys. Res.*, *111*, D06108, doi:10.1029/2005JD006283.
- McCormack, J. P. (2003), The influence of the 11-year solar cycle on the quasi-biennial oscillation, *Geophys. Res. Lett.*, *30*(22), 2162, doi:10.1029/2003GL018314.
- McCormack, J. P., D. E. Siskind, and L. L. Hood (2007), The solar-QBO interaction and its impact on stratospheric ozone in a zonally averaged photochemical-transport model of the middle atmosphere, *J. Geophys. Res.*, *112*, D16109, doi:10.1029/2006JD008369.
- Meehl, G. A., W. M. Washington, T. M. L. Wigley, J. M. Arblaster, and A. Dai (2003), Solar and greenhouse gas forcing and climate response in the twentieth century, *J. Clim.*, *16*, 426–444.

- NAG (1999), NAG Library, Mark 19, Copyright National Algorithms Group Limited.
- Neu, J. L., and R. A. Plumb (1999), Age of air in a "leaky pipe" model of stratospheric transport, *J. Geophys. Res.*, *104*, 19,243–19,255.
- Nissen, K. M., K. Matthes, U. Langematz, and B. Mayer (2007), Towards a better representation of the solar cycle in general circulation models, *Atmos. Chem. Phys.*, *7*, 5391–5400.
- Randel, W. J., and F. Wu (2007), A stratospheric ozone profile data set for 1979–2005: Variability, trends, and comparisons with column ozone data, *J. Geophys. Res.*, *112*, D06313, doi:10.1029/2006JD007339.
- Rinsland, C. P., C. Boone, R. Nassar, K. Walker, P. Bernath, J. C. McConnell, and L. Chiou (2005), Atmospheric chemistry Experiment (ACE) Arctic stratospheric measurements of NO_x during February and March 2004: Impact of intense solar flares, *Geophys. Res. Lett.*, *32*, L16S05, doi:10.1029/2005GL022425.
- Rozanov, E., L. Callis, M. Schlesinger, F. Yang, N. Andronova, and V. Zubov (2005a), Atmospheric response to NO_x source due to energetic electron precipitation, *Geophys. Res. Lett.*, *32*, L14811, doi:10.1029/2005GL023041.
- Rozanov, E., M. Schraner, C. Schnadt, T. Egorova, M. Wild, A. Ohmura, V. Zubov, W. Schmutz, and T. Peter (2005b), Assessment of the ozone and temperature variability during 1979–1993 with the chemistry-climate model SOCOL, *Adv. Space Res.*, *35*(8), 1375–1384.
- Rozanov, E., M. Schraner, T. Egorova, A. Ohmura, M. Wild, W. Schmutz, and T. Peter (2005c), Solar signal in atmospheric ozone, temperature and dynamics simulated with CCM SOCOL in transient mode, *Mem. S.A. It.*, *76*, 876–879.
- Scaife, A. A., J. Austin, N. Butchart, M. Keil, S. Pawson, J. Nash, and I. N. James (2000), Seasonal and interannual variability of the stratosphere diagnosed from UKMO TOVS analyses, *Q.J.R. Meteorol. Soc.*, *126*, 2585–2604.
- Schmidt, H., and G. P. Brasseur (2006), The response of the middle atmosphere to solar cycle forcing in the Hamburg model of the neutral and ionized atmosphere, *Space Sci. Rev.*, *125*, 345–356.
- Schmidt, H., G. Brasseur, M. Charron, E. Manzini, M. A. Giorgetta, V. Fomichev, D. Kinnison, D. Marsh, and S. Walters (2006), The HAMMONIA chemistry climate model: Sensitivity of the mesopause region to the 11-year solar cycle and CO_2 doubling, *J. Clim.*, *19*, 903–931.
- Shibata, K., and M. Deushi (2005), Partitioning between resolved wave forcing and unresolved gravity wave forcing to the quasi-biennial oscillation as revealed with a coupled chemistry-climate model, *Geophys. Res. Lett.*, *32*, L12820, doi:10.1029/2005GL022885.
- Shibata, K., and K. Kodera (2005), Simulation of radiative and dynamical responses of the middle atmosphere to the 11-year solar cycle, *J. Atmos. Sol. Terr. Phys.*, *67*, 125–143, doi:10.1016/j.jastp.2004.07.022.
- Shibata, K., M. Deushi, T. T. Sekiyama, and H. Yoshimura (2005), Development of an MRI chemical transport model for the study of stratospheric chemistry, *Pap. Meteorol. Geophys.*, *55*, 75–119.
- Shindell, D., D. Rind, N. Balachandran, J. Lean, and P. Lonergan (1999), Solar cycle variability, ozone, and climate, *Science*, *284*, 305–308.
- Shindell, D., G. A. Schmidt, R. L. Miller, and M. E. Mann (2003), Volcanic and solar forcing of climate change during the preindustrial era, *J. Clim.*, *16*, 4094–4107.
- Shine, K. P., J. J. Barnett, and W. J. Randel (2008), Temperature trends derived from Stratospheric Sounding Unit radiances: The effect of increasing CO_2 on the weighting function, *Geophys. Res. Lett.*, *35*, L02710, doi:10.1029/2007GL032218.
- Soukharev, B. E., and L. L. Hood (2006), The solar cycle variation of stratospheric ozone: Multiple regression analysis of long-term satellite data sets and comparisons with models, *J. Geophys. Res.*, *111*, D20314, doi:10.1029/2006JD007107.
- Steil, B., C. Brühl, E. Manzini, P. J. Crutzen, J. Lelieveld, P. J. Rasch, E. Roeckner, and K. Krüger (2003), A new interactive chemistry-climate model: 1. Present-day climatology and interannual variability of the middle atmosphere using the model and 9 years of HALOE/UAARS data, *J. Geophys. Res.*, *108*(D9), 4290, doi:10.1029/2002JD002971.
- Steinbrecht, W., et al. (2006), Interannual variation patterns of total ozone and lower stratospheric temperature in observations and model simulations, *Atmos. Chem. Phys.*, *6*, 349–374.
- Stolarski, R. S., A. R. Douglass, S. Steenrod, and S. Pawson (2006), Trends in stratospheric ozone: Lessons learned from a 3d chemical transport model, *J. Atmos. Sci.*, *63*, 1028–1041.
- Strobel, D. F. (1978), Parameterization of the atmospheric heating rate from 15 to 120 km due to O_2 and O_3 absorption of solar radiation, *J. Geophys. Res.*, *83*, 6225–6230.
- Struthers, H., K. Kreher, J. Austin, R. Schofield, G. Bodeker, P. Johnston, H. Shiona, and A. Thomas (2004), Changes in the rate of increase of NO_2 as predicted by a three-dimensional coupled chemistry-climate model, *Atmos. Chem. Phys.*, *4*, 2227–2239.
- Thomason, L. W., and L. R. Poole (1997), A global climatology of stratospheric aerosol surface area density deduced from Stratospheric Aerosol and Gas Experiment II measurements: 1984–1994, *J. Geophys. Res.*, *102*, 8967–8976.
- Tian, W., and M. P. Chipperfield (2005), A new coupled chemistry-climate model for the stratosphere: the importance of coupling for future O_3 -climate predictions, *Q.J.R. Meteorol. Soc.*, *131*, 281–304.
- Tiao, G. C., G. C. Reinsel, D. Xu, J. H. Pedrick, X. Zhu, A. J. Miller, J. J. DeLuisi, C. L. Mateer, and D. J. Wuebbles (1990), Effects of autocorrelation and temporal sampling schemes on estimates of trend and spatial correlation, *J. Geophys. Res.*, *95*, 20,507–20,517.
- Tourpali, K., C. J. E. Schuurmans, R. van Dorland, B. Steil, and C. Brühl (2003), Stratospheric and tropospheric response to enhanced solar UV radiation: A model study, *Geophys. Res. Lett.*, *30*(5), 1231, doi:10.1029/2002GL016650.
- Tourpali, K., C. S. Zerefos, D. S. Balis, and A. F. Bais (2007), The 11-year solar cycle in stratospheric ozone: comparison between Umkehr and SBUV v8 and effects on surface erythral irradiance, *J. Geophys. Res.*, *112*, D12306, doi:10.1029/2006JD007760.
- White, W. B., M. D. Dettinger, and D. R. Cayan (2003), Sources of global warming of the upper ocean on decadal period scales, *J. Geophys. Res.*, *108*(C8), 3248, doi:10.1029/2002JC001396.
- WMO (2007), Stratospheric processes: Observations and interpretation, WMO Rep. 50, Global Ozone Res. and Monit. Proj., Geneva.
- Yoshimori, M., T. M. Stocker, C. C. Raible, and M. Renold (2005), Externally forced and internal variability in ensemble climate simulations of the Maunder minimum, *J. Clim.*, *18*, 4253–4270.
- Zerefos, C. S., K. Tourpali, B. R. Bojkov, and D. S. Balis (1997), Solar activity-total ozone relationships: observations and model studies with heterogeneous chemistry, *J. Geophys. Res.*, *102*, 1561–1569.
- H. Akiyoshi and T. Nagashima, National Institute for Environmental Studies, 16-2 Onogawa, Tsukuba-shi, Ibaraki 305-0053, Japan.
- J. Austin, Geophysical Fluid Dynamics Laboratory, Princeton, NJ 08542-0308, USA. (john.austin@noaa.gov)
- S. Bekki and F. Lott, UPMC Univ Paris 06, CNRS, SA-IPSL, B.102, 4, Place Jussieu, 75252 Paris, CEDEX, France.
- G. Bodeker and H. Struthers, NIWA, Private Bag 50061, Omakau 9352, Central Otago, New Zealand.
- C. Brühl, Max Planck Institut für Chemie, P.O. Box 3060, 55020 Mainz, Germany.
- N. Butchart, Met Office Climate Research Division, FitzRoy Road, Exeter, Devon EX1 3PB, UK.
- M. Chipperfield and W. Tian, Institute for Atmospheric Science, University of Leeds, Leeds LS2 9JT, UK.
- M. Deushi and K. Shibata, Meteorological Research Institute, 1-1 Nagamine, Tsukuba, Ibaraki 305-0052, Japan.
- V. I. Fomichev, Department of Earth and Space Science and Engineering, York University, 4700 Keele Street, Toronto, ON M3J 1P3, Canada.
- M. A. Giorgetta, Max Planck Institute for Meteorology, Bundesstr. 53, 20146 Hamburg, Germany.
- L. Gray, NCAS Centre for Global Atmospheric Modelling, Meteorology Department, Reading University, Earley Gate, P.O. Box 243, Reading RG6 6BB, UK.
- K. Kodera, Graduate School of Environmental Studies, Nagoya University, Kankyo Sogo-kan, 401 Furo-cho, Chikusa, Nagoya 464-8601, Japan.
- E. Manzini, Istituto Nazionale di Geofisica e Vulcanologia and Centro Euro-Mediterraneo per i Cambiamenti Climatici, 40128 Bologna, Italy.
- D. Marsh, Atmospheric Chemistry Division, National Center for Atmospheric Research, P.O. Box 3000, Boulder, CO 80307-3000, USA.
- K. Matthes, Institut für Meteorologie, Freie Universität Berlin, Carl-Heinrich-Becker-Weg 6-10, 12165 Berlin, Germany.
- E. Rozanov, PMOD/WRC and IAC ETHZ, Dorfstrasse 33, CH-7260 Davos Dorf, Switzerland.
- R. S. Stolarski, NASA Goddard Space Flight Center, Code 613.3, Greenbelt, MD 20771, USA.
- K. Tourpali, Laboratory of Atmospheric Physics, Aristotle University of Thessaloniki, P.O. Box 149, 20006 Thessaloniki, Greece.